

NASA Contractor Report 4767

# Documentation of Atmospheric Conditions During Observed Rising Aircraft Wakes

---

*J. Allen Zak*  
*ViGYAN, Inc. • Hampton, Virginia*

*William G. Rodgers, Jr.*  
*Lockheed Martin Engineering and Sciences • Hampton, Virginia*

Prepared for Langley Research Center  
under Contract NAS1-96014

April 1997

Available electronically at the following URL address: <http://techreports.larc.nasa.gov/ltrs/ltrs.html>

Printed copies available from the following:

NASA Center for AeroSpace Information  
800 Elkridge Landing Road  
Linthicum Heights, MD 21090-2934  
(301) 621-0390

National Technical Information Service (NTIS)  
5285 Port Royal Road  
Springfield, VA 22161-2171  
(703) 487-4650

## Table of Contents

1.	Introduction and Background.....	1
2.	Potential Rising Vortex Causes .....	2
3.	Flight Experiments .....	2
4.	Data Collection.....	3
4.1.	Aircraft Data .....	3
4.2.	Other Meteorological Data.....	4
5.	Data Processing .....	5
5.1.	Altitude data .....	5
5.2.	OV-10 Flight and Meteorological Parameters .....	5
5.3.	Radiosonde data.....	5
6.	Results.....	6
6.1.	Meteorology for Flight Days .....	6
6.2.	Wake Behavior.....	7
6.2.1.	Sinking Vortices .....	8
6.2.2.	Level or Rising Vortices .....	8
6.2.3.	Oscillating Vortices .....	9
7.	Conclusions .....	9
	References.....	10

## List of Tables

Table 1.	Flight Summary .....	11
Table 2.	Data Available.....	11
Table 3.	OV-10 Parameters.....	11
Table 4.	Other Meteorological Data Available.....	11
Table 5.	Data Summary for Rising Vortex Research.....	12
Table 6.	Data Summary for Sinking Vortices .....	14
Table 7.	Data Summary for Rising Vortices .....	15
Table 8.	Data Summary for Wakes with Large Oscillations .....	16

## List of Figures

Figure 1.	Wake Vortex Flow Field.....	17
Figure 2.	Wake Vortex Descent Rates .....	17
Figure 3.	Video Frame of OV-10 Drifting Behind the C130 .....	18
Figure 4a.	Video Frame of OV-10 Level with the Starboard Vortex .....	18
Figure 4b.	Video Frame of OV-10 Penetrating Starboard Vortex.....	18
Figure 4c.	Video Frame of OV-10 Below the Port Vortex.....	18
Figure 5.	OV-10 Experimental Configuration.....	19
Figure 6a.	Surface Weather Map for October 19, 1995, 1200 GMT.....	20
Figure 6b.	850 Hectopascal Weather Map for October 19, 1995, 1200 .....	20
Figure 6c.	Balloon Sounding for October 19, 1995, 1400 GMT.....	20
Figure 6d.	Balloon Sounding for October 19, 1995, 1750 GMT.....	21
Figure 6e.	Balloon Sounding for October 19, 1995, 2046 GMT.....	21
Figure 7a.	Surface Weather Map for October 26, 1995, 1200 GMT.....	22
Figure 7b.	850 Hectopascal Weather Map for October 26, 1995, 1200 .....	22
Figure 7c.	Balloon Sounding for October 26, 1995, 1131 GMT.....	22
Figure 8a.	Surface Weather Map for November 6, 1995, 1200 GMT .....	23
Figure 8b.	850 Hectopascal Weather Map for November 6, 1995, 1200.....	23
Figure 8c.	Balloon Sounding for November 6, 1995, 1730 GMT .....	23
Figure 9a.	Surface Weather Map for November 8, 1995, 1200 GMT .....	24
Figure 9b.	850 Hectopascal Weather Map for November 8, 1995, 1200.....	24
Figure 9c.	Balloon Sounding for November 8, 1995, 1600 GMT .....	24
Figure 10a.	Surface Weather Map for November 9, 1995, 1200 GMT .....	25
Figure 10b.	850 Hectopascal Weather Map for November 9,1995, 1200.....	25
Figure 10c.	Balloon Sounding for November 9, 1995, 1843 GMT .....	25
Figure 11.	C130 and OV-10 GPS Altitude for Flight 551 at Run Times Shown.....	26
Figure 12.	C130 and OV-10 GPS Altitude for Flight 552 at Run Times Shown .....	27
Figure 13.	C130 and OV-10 GPS Altitude for Flight 553 at Run Times Shown.....	29
Figure 14.	C130 and OV-10 GPS Altitude for Flight 555 at Run Times Shown.....	30
Figure 15.	C130 and OV-10 GPS Altitude for Flight 556 at Run Times Shown.....	31
Figure 16.	C130 and OV-10 GPS Altitude for Flight 557 at Run Times Shown.....	33
Figure 17.	Video Frames From Different Times of the C130 Wake Vortex Smoke Signature .	34

## **Appendices**

### **Appendix A - Balloon Sounding Data For Wake Decay Flight Days**

Because of the extensive data contained in this appendix, it has not been included in the printed copy of this report but is available from the Langley Technical Report Server (LTRS). Open the files with the following Uniform Resource Locator (URL):

<ftp://techreports.larc.nasa.gov/pub/techreports/larc/1997/cr/NASA-97-cr4767appA.txt>

### **Appendix B - Altitude Comparison Data**

Because of the extensive data contained in this appendix, it has not been included in the printed copy of this report but is available from the Langley Technical Report Server (LTRS). Open the files with the following Uniform Resource Locator (URL):

<ftp://techreports.larc.nasa.gov/pub/techreports/larc/1997/cr/NASA-97-cr4767appB.txt>

## Abstract

Flight tests were conducted in the fall of 1995 off the coast of Wallops Island, Virginia in order to determine characteristics of wake vortices at flight altitudes. A NASA Wallops Flight Facility C130 aircraft equipped with smoke generators produced visible wakes at altitudes ranging from 775 to 2225 m in a variety of atmospheric conditions, orientations (head wind, cross wind), and airspeeds. Meteorological and aircraft parameters were collected continuously from a Langley Research Center OV-10A aircraft as it flew alongside and through the wake vortices at varying distances behind the C130. Meteorological data were also obtained from special balloon observations made at Wallops. Differential GPS capabilities were on each aircraft from which accurate altitude profiles were obtained. Vortices were observed to rise at distances beyond a mile behind the C130. The maximum altitude was 150 m above the C130 in a near neutral atmosphere with significant turbulence. This occurred from large vertical oscillations in the wakes. There were several cases when vortices did not descend after a very short initial period and remained near generation altitude in a variety of moderately stable atmospheres and wind shears.

### 1. Introduction and Background

This research is a continuing effort on the part of the NASA Langley Research Center (LaRC), the Federal Aviation Administration (FAA) and other government agencies to understand the complex behavior of wake vortices in a variety of atmospheric conditions. A significant effort is now underway at LaRC as part of a NASA Terminal Area Productivity Program to determine safe operating spacing between arriving aircraft. Such spacing is now conservatively determined by aircraft size/weight classes between lead and following aircraft pairs. If this spacing can be safely reduced under certain atmospheric conditions, then capacity can be increased at many airports throughout the world. The Aircraft Vortex Spacing System (AVOSS) (ref. 1) is striving to determine this safe spacing based on observed and predicted atmospheric conditions. Understanding atmospheric wake vortex interaction is, therefore, on a critical path in this endeavor.

Wake vortices are manifestations of flight. Two areas of large pressure gradients are created at the wings. Counter rotating air flows develop behind the wing tips as shown in figure 1. These present a hazard to aviation in that the rolling moment induced by the inadvertent penetration of a vortex can exceed the roll control authority of the penetrating

aircraft. Vortex strength initially depends on three factors: the weight, wing span and airspeed of the generating aircraft. Other factors involved are wing configuration and flight attitude. Vortices descend after initial formation. Current training material states that this descent continues for the first 5 nm then levels off (ref. 2). Initial descent rates are stated to be typically 300 to 500 feet per minute for the first 30 seconds. As shown in figure 2, vortices then are expected to continue to descend at a slower rate and eventually stop descending at between 500 to 900 ft below the generating aircraft. Pilots are taught, therefore, to fly "at or above the preceding aircraft's flight path altering course as necessary to avoid the area behind and below the generating aircraft." (ref. 3).

The NASA Langley Research Center embarked on a series of wake vortex flight tests during the fall of 1995 off the coast of Wallops Island, VA. The purpose of these tests was to collect data on wake vortex decay, on vortex-aircraft interaction, and for in-flight wake detection. During some on these flights, pilots reported rising wakes. Understanding conditions that can lead to rising vortices is essential to the success of AVOSS. Therefore, the purpose of this research was to confirm if wake vortices generated by a C130 NASA aircraft rise at flight altitudes and to document the

meteorology associated with these occurrences. Other characteristics of the vortices such as strength and decay will be candidates for future research.

The atmosphere plays a significant role in the movement and decay as well as in the general behavior of the vortex pair following initial descent. This research documents some of these atmospheric effects and identifies some cases where the vortex actually rises to an altitude above the generating aircraft in level flight outside of ground effects.

## 2. Potential Rising Vortex Causes

The effects of atmospheric stratification on aircraft wake vortices have been investigated in the past (ref. 4, 5, 6). The vortex pair descends and warms adiabatically owing to compression. The vortices can then achieve a temperature warmer than the environment, and upward buoyancy forces can theoretically counteract and eventually exceed the downward momentum if the stable stratification is very strong. The magnitude of the buoyancy force can be measured by the Brunt-Väisälä (B-V) frequency (ref. 6) squared, which is the numerator in the Richardson Number, a frequently used measure of atmospheric turbulence:

$$(B-V)^2 = \frac{g}{\theta} \frac{\partial \theta}{\partial Z}$$

where  $g$  is the acceleration of gravity,  $\theta$  the potential temperature, and  $Z$  the altitude.

Wind shear also plays a role. Most recently, Proctor, et. al., have shown in vortex simulations that nonlinear cross wind profiles can arrest the descent of vortex pairs and that this nonlinearity was more important than the shear itself (ref. 7).

Vortices can be imbedded in strong vertical currents, especially during the afternoon on convectively active days. Such “thermals” can exceed 1 m/s (several hundred feet per minute) on thermally active days as any soaring enthusiast can confirm. These conditions can be inferred from measures of atmospheric stability (ref. 8) from balloon soundings.

Rising motion can be imparted to the vortex pair due to mountain waves or gravity waves propagating along atmospheric discontinuities such as inversions. Gravity waves from mountains in NW Montana have been reported to affect the initiation of thunderstorms as far as several hundred kilometers downstream (ref. 9).

Finally, atmospheric turbulence can enhance vortex instabilities that can be manifest in oscillatory motions (ref. 10). Such features as vortex bursting, Crow instability, and linking have been observed and described in the past (see ref. 11 for a summary). Vertical sinusoids can be a potential source of vortices ascending above flight generation altitude.

The above is a simplification for discussion purposes. It is likely on any given day that several of these effects and others, perhaps not yet identified, can act on the vortices at any given time and place in very complex ways. Some of these effects will be discussed in the context of results found in this research.

## 3. Flight Experiments

The NASA Langley Research Center with the cooperation of the NASA Wallops Flight Facility conducted a series of wake decay flights off the coast of Wallops Island, VA. A NASA C130 aircraft acted as the wake-generation aircraft. It was equipped with wing

tip smoke generators to make the vortices visible to the trailing aircraft, a NASA OV-10A. The OV-10 was instrumented to measure and record atmospheric temperature, dew point, winds and turbulence as well as aircraft motion and fundamental aircraft parameters. More details will be provided under Data Collection.

There were six wake decay missions flown in October and November 1995. Table 1 lists the date, times, flight altitudes, general weather conditions, and vortex characteristics for each. Flight altitudes ranged from 800 m to 2200 m (about 2500 to 7000 ft) and were planned to coincide with meteorological events such as inversions whenever possible. The OV-10 collected a vertical sample of meteorological data at the beginning of each mission in order to determine gross atmospheric features such as inversion heights and strengths. This then led to selection of working altitudes such as below, in, or above the inversion. Horizontal and vertical atmospheric sampling continued in selected atmospheric regions near the working altitudes. A mission consisted of a series of runs where the C130 and OV-10 would fly level and parallel at a chosen airspeed, heading, and altitude. The OV-10 would reduce airspeed to drift behind the C130 and would start penetrating the vortices from about 1 mile behind to as far as 7 miles behind if the vortices remained visible that long. Figure 3 is a frame from the tail camera video showing the OV-10 just beginning to drift behind the C130. As the OV-10 entered the vortex from either the port or starboard side, the aircraft would descend below the track of the opposite vortex due to the vortex circulation (downward between the vortices). Figure 4 is a sequence showing the OV-10 level with the starboard vortex just before penetration (4a), in the starboard vortex (4b), then falling down under the port vortex (4c).

The OV-10 would continue a series of penetrations at varying times (distances) behind the C130 to accumulate data on vortex and atmospheric characteristics at different vortex ages. This sequence would then be repeated for a different flight altitude, different orientation (head wind (HW), tail wind (TW), cross wind (CW)), or different airspeed. If both smoke generators were operating, the penetration would be sequenced between the port and starboard side: starboard vortex penetrated then below the port vortex followed by level with and penetration of the port vortex then below the starboard vortex. If only one smoke generator were operating, the OV-10 would penetrate just the visible vortex, but from either side. The pilots reported the strongest roll upsets when penetrating from the inside (between the vortices) out. Needless to say, in the wake turbulence behind the C130, the pilot had a challenging task to find the center of the vortex when air at the vortex boundary was always moving up or down as he approached the vortex.

## 4. Data Collection

Data for this study were collected from the C130, and OV-10 aircraft and crew, synoptic weather charts, routine upper air soundings, and special balloon soundings taken for these tests by NASA Wallops Flight Facility, Flight Ops personnel.

### 4.1. Aircraft Data

The experimental configuration of the OV-10A is shown in figure 5. A discussion of each sensor system and its output can be found in reference 12.

Of special significance was a custom-built data acquisition system capable of recording about two hours of data for one mission at a rate

sufficiently high to characterize high-frequency atmospheric turbulence. Also critical to this study were Ashtech differential Global Positioning System (GPS) receivers on both the C130 and OV-10 with associated ground stations at NASA Langley and NASA Wallops from which highly accurate positions (longitudinal, lateral and vertical) could be obtained. On these flights the data rate for the Rosemount probe on the graphite-epoxy nose boom from which wind components were calculated was 128 samples per second. Measurement rates from the other sensors ranged from 4 to 32 samples per second. Temperature and dew point were recorded at 8 samples per second. The tail camera provided video tape documentation of each mission along with audio tracks of pilot and/or researcher comments as well as an IRIG time code at the top of each frame. Pilot logs were also available from the C130 and OV-10 flight crews. The C130 has a wing span of 40.2 m (132 ft) and its weight ranged from 44,452 kg to 47,627 kg (98,000 lb to 105,000 lb) during these missions.

For this study the temperature, dew point, wind components, GPS positions, especially altitude, and turbulent wind components were used in conjunction with the OV-10 video tapes, and pilot logs to characterize the height of the vortex encounters as well as pertinent atmospheric conditions and vortex behavior. A summary of major aircraft data sources available is presented in Table 2, and Table 3 shows the parameters collected on the OV-10. Note that in Table 2 the Ashtech differential GPS was not available on the C130 for Flights 552 and 553. Also note that there was no Ashtech GPS on the OV-10 until Flight 555. There was excellent agreement in comparisons of pressure altitude, Ashtech GPS, and Honeywell GPS when they were all available. Therefore, for the earlier flights, the Honeywell non-differential GPS was used for

the OV-10 flight altitude. Finally, there was little or no video available for Flights 552 and 555.

## **4.2. Other Meteorological Data**

It is important in any study of wake vortex phenomena in the atmosphere that the ambient meteorological conditions be determined. It was stated earlier that atmospheric stratification or vertical temperature and moisture gradients, vertical wind shear, and turbulence can play significant roles in wake vortex behavior. Special upper air balloon radiosonde observations were taken during each flight to provide ambient vertical temperature, moisture and wind profiles. Radiosonde packages (VIZ W-9000 MK-2) with cross-chain Loran were used with a 300 gm balloon. Ascent rate was 305 m/min for the special soundings. In addition, Wallops personnel take upper-air radiosonde observations twice daily at 0000 and 1200 GMT for the National Weather Service as part of the National Network. These were 600 gm balloons with an ascent rate of 366 m/min. The special data for Flights 551 and 552 were available at either 2 second or 5 second resolution corresponding to 10 and 25 meter vertical resolution respectively; but for the other flights (and for the network soundings) the vertical resolution was about 750 m for temperature and dew point and 300 m for winds. If there were significant temperature features, more resolution was available. The wind information output at the 2 or 5 second rate was a running 6 second average.

The meteorological measurements from the balloon as well as from the OV-10 must be understood in the context of the larger scale features of the atmosphere. Therefore, the surface and 850 hectopascal weather maps were obtained for each flight day. A summary

of other meteorological data available for this study is shown in Table 4.

## 5. Data Processing

Processing of altitude data, aircraft speed and heading, OV-10 meteorological data, and radiosonde balloon data provided the basis for this study.

### 5.1. Altitude data

It was possible to obtain the flight altitudes of the C130 and its wakes as a function of time or distance. Software written by the LaRC Vehicle Dynamics Branch was modified to calculate range of the OV-10 from the C130 as a function of time. Output was altitude vs. time for both the C130 when it generated the vortices and the OV-10 when it penetrated them at various distances behind. In other words, altitude is shown as a function of time for the OV-10, but altitude for the C130 is shown for a time which was adjusted for the age of the vortex encountered.

### 5.2. OV-10 Flight and Meteorological Parameters

One second averages for all parameters were computed from their original measurement rates. Aircraft position (x, y, and z representing the E-W, N-S and height components respectively) was plotted as a function of time for all runs. Heading, pressure, temperature, dew point, and winds were also plotted as a function of time. Wind was shown as direction (from true north), speed, and the three orthogonal components, u, v, and w corresponding to x, y, and z respectively, all as a function of time. The data were separated into “abeam” when the OV-10 was flying parallel to the C130 at the beginning of each run, “penetration”, when the

OV-10 began to enter the wakes, and level weather segments. Further processing was done for the abeam and level weather segments to provide statistics such as minimum, maximum, means and variances. Altitude and all the meteorological parameters were included in the statistics. In addition, cross correlations were computed among temperature, dew point, and u, v, and w fluctuations of the high frequency measurements from the mean value during the time of the level flight segment. One correlation combination was computed to represent the turbulent kinetic energy (TKE) of the environment as follows:

$$TKE = \frac{u' u' + v' v' + w' w'}{2}$$

where the primes indicate deviation from the 2 minute mean.

### 5.3. Radiosonde data

Standard pre-processing was done at the Wallops Flight Facility to provide temperature, dew point, wind direction, and speed for each pressure (altitude). The potential temperature was calculated for visualization of stability. All parameters (potential temperature, temperature, dew point, and wind) were plotted as a function of altitude for each balloon sounding time. The mean lapse rates (potential temperature change with altitude), where positive is increasing temperature with height, and cross wind shear from about 50 meters above the vortex altitude to 75 meters below were calculated for every run. This is opposite to the usual meteorological terminology for positive and negative lapse rates where the lapse rate is defined with a negative sign. When the potential temperature increases with

height, the atmosphere is stable<sup>1</sup>. B-V frequency was also calculated for each run. Finally, the bottom and top of temperature inversions and maximum strength were identified from the changing lapse rate structure for each sounding. The data for all the balloon soundings are included in Appendix A.

## 6. Results

A discussion of the most important characteristics of vortex behavior and associated meteorology will be the focus of this section. First, the meteorology for each flight day will be discussed. Next will be the discussion of the combined vortex generation altitude and altitude of penetration at various vortex ages and distances behind the generating aircraft. Finally, the meteorology and vortex behavior will be presented for times of sinking vortices, steady or rising vortices, and disturbed vortices. Cause-effect mechanisms will be included when possible.

### 6.1. Meteorology for Flight Days

There were no extraordinary meteorological events occurring on any wake encounter day. Flight tests were planned and executed when no adverse weather was threatening the test region. Figure 6 shows the surface weather map (6a) and 850 hectopascal analysis (6b) for October 19, 1995 whereas Figure 6c, d, and e show plots of the balloon soundings at the times indicated. There were two flights on this day. High pressure dominated the region with clear skies in the morning and scattered cumulus clouds in the afternoon. The high pressure aloft created subsiding air which was indicated as a weak inversion and generally stable conditions in the balloon soundings.

---

<sup>1</sup> or more precisely, conditionally unstable until it exceeds the moist adiabatic lapse rate

Stability at flight altitudes generally decreased in the afternoon except for Flight 552, runs 8 and 9, which were in the top of a rather weak inversion layer. All the other runs were above the inversion but still in stable air. Winds at flight altitudes were generally SW 5-8 m/s. There was little turbulence with some cross wind shear on some runs. The next flight day, October 26, was very similar (Fig. 7a, b) with even higher pressure dominating the region. The sounding (Fig. 7c) reflects a stronger inversion. Three of the runs (11, 12, and 13) were at the top of the inversion where there was a very stable atmosphere. Flight level winds were Westerly 5-12 m/s with stronger cross wind shears at the inversion top. There were scattered clouds and haze trapped below the inversion. High pressure at the surface was the major feature on the next flight day, November 6 (Fig. 8a, b). Again, the sounding (Fig. 8c) shows the characteristic inversion and stability. Lapse rates for all flight altitudes were closer to neutral than on any prior flights, however, skies remained clear. Winds aloft and shears remained light, but turbulence levels increased from the earlier flights. There was a significant difference for the next two flight days. A strong cold front moved through the region early on November 8 with a strong NW flow from the surface to 3 km altitude and strong cold air advection (Fig. 9 a, b). This combination produced a well mixed lower atmosphere with neutral stability and significant turbulence. The sounding shown in Figure 9c reflects the neutral stability below 1300 m. All the runs were in this well-mixed, turbulent layer. Winds were 12 m/s at flight altitude with a trajectory perpendicular to the mountains in Western Maryland. There were clouds slightly above the flight altitude of 900 m (3,000 ft), some of which had vertical development and looked like towering cumulus in the video. Conditions on the last flight day, November 9, 1995, were similar at flight level, but there was increased stability

aloft from a building surface high pressure system that moved into the area from the West (Fig. 10a, b, and c).

The above meteorological conditions will be called upon to help explain some characteristics of the wakes discussed next.

## 6.2. Wake Behavior

Results for every flight and run are summarized in Table 5. All the important information from the processing and analyses of all the data are presented in this table. In the discussion that follows, it is not necessary (except to confirm a table entry) to refer to either the weather maps or soundings. A series of plots was generated for superimposed C130 altitude and OV-10 altitude. The C130 altitude was plotted at the time of vortex generation. The OV-10 distance (in nautical miles) behind the C130 is shown in each plot. These plots for all flights and runs for which data were available are shown in Figures 11-16, one sequence of runs for each flight. The altitude data for these flights are included in Appendix B. OV-10 vortex penetrations and basic vortex behavior (sink, rise, or steady) can be seen by visual inspection. One can see the change in altitude of the OV-10 as it is penetrating the vortices after about one mile behind the C130: descent upon penetration, then climb for the next penetration. Figure 11a (run 06), for example, shows the altitude changes for the OV-10 after it started vortex penetrations at about 1 1/4 miles behind the C130 at 1332 GMT. The plot shows a steady descent to the vortices until about 4 1/2 miles behind the C130. In Figure 11c (run 13) one can see the altitude of the C130 changing (top curve) so that the behavior of the vortex, showing to be steady at 1500 m between 1442 and 1443 GMT, would have actually been descending because the C130 was rising as it was generating the vortices. The altitude

scales are the same for all plots, but the time scales (abscissa) change depending on how long the vortices could be seen. Unfortunately, for Flights 553 and 555 there was no altitude available for the C130 so we can only assume it was level in interpreting vortex ascent or descent. There was evidence from pilot comments that the autopilot on the C130 was not working properly for portions of Flights 551 and 552 as can be seen in the altitude plots for some of these runs.

There were some limitations, however, that could affect the results. The lack of video confirmation and pilot comments for Flights 552 and 555 prevented confirmation of wake behavior, and the absence of altitude information for the wake generating C130 makes the determination of vortex behavior (sinking, steady, or rising) speculative. There were also some inconsistencies noted in pilot altitude calls from his altimeter with the GPS altitude plots. The GPS data are assumed to be correct. Vertical wind measurements appear to have a positive bias of 0.5 m/s, a large number for atmospheric vertical motion, so this information is only used in a relative sense. There were some differences in horizontal wind measurements between the OV-10, C130, and balloons, but none beyond that reasonably expected in the atmosphere. The only corrections made in the data presented in Table 5 were for differences in Earth Geoid references for the GPS systems, constants in both cases. Change in potential temperature with height was also graphically determined from balloon potential temperature plots. The wind shear information presented in Table 5 was calculated from the sounding taken at a different time and location from the wake encounter flights. When there were two soundings bracketing a flight, some interpolation was performed. Furthermore, there was considerable smoothing in the vertical winds, so that shears are not very

representative of those that may have contributed to vortex behavior for any of the runs. For this reason other parameters such as Richardson Number used by many to assess atmospheric turbulence is not calculated since it includes the wind components squared in the denominator.

Since a major goal of this study was to determine whether or not wakes rise at flight altitudes, the sequence of plots in Figure 11 through 16 is critical to the outcome.

During flights on October 19 (551 and 552) there are only small differences between generation altitude and vortex altitude among the runs. For 553 and 555 there was no C130 altitude so the C130 was assumed to be in level flight. Nevertheless, those runs in which the vortices predominantly descended and those where there was very little or no descent beyond an initial period were identified and separated for discussion purposes. Because vortices on the last two days underwent significant vertical and horizontal undulations, they were also separated. Each group will be discussed below.

**6.2.1. Sinking Vortices.** Vortices appeared to be predominantly sinking during their lifetime (represented by their smoke trail) for 551 run 06, 552 runs 05 and 10, 553 run 8, and 555 run 03 and 04. These cases are extracted from Table 5 and summarized in Table 6. Note that the average potential temperature lapse rate was 0.48 degrees C/100 m and B-V frequency was 0.0127/s for the sinking cases. The lower lapse rate represents fewer upward motion forces, as would be expected, than for the level to rising cases presented next. Also of interest are the two runs separated by 45 minutes in Flight 551 (runs 06 and 10). Both were head wind cases and at the same altitude. The former sank significantly, whereas the latter remained

nearly level. Notwithstanding wind shear effects which may not be adequately represented, the biggest difference was that the airspeed of the C130 was 90 m/s for run 10 and 60 m/s for run 06. The other difference is a slight increase in stability, therefore buoyancy, for this later flight as interpolated between the two closest balloon soundings.

For Flight 552 there also was a sinking vortex followed by a steady vortex. The only difference here was that run 05 was in a tail wind configuration and run 06 was a cross wind. Therefore, the cross wind shear for run 06 was three times the value of the first run (run 05), or 0.3 compared to 0.1 m/s per 100 m. There did not seem to be any other correlations with orientation (head wind, tail wind, cross wind) or anything else separating these sinking vortex cases from the others.

**6.2.2. Level or Rising Vortices** These cases are spread throughout the flights as shown in Table 7. The average lapse rate increased to 1.03 degrees C/100 m and the corresponding average B-V frequency (0.0177) was higher. There are individual exceptions, however. Flight 551 run 10 and 552 run 6 were already discussed. There may be other factors involved such as wind shear and/or interactions of all the effects, some of which cannot be adequately determined. The assumption that the C130 was steady for Flight 553 may also be incorrect. It is interesting to note that the one case documented from the GPS plots, 552 run 9, when the vortices rose above the generating altitude, involved a flight near the top of the inversion in the region of maximum positive lapse rate. There were other cases when vortices rose above the wake generation altitude, but these involved large sinusoidal oscillations to be discussed next.

**6.2.3. Oscillating Vortices** Strong horizontal and vertical oscillations began to appear in the vortices on the last two flight days as close as one-fourth mile behind the C130. Some of these oscillations are shown in Figure 17 as the OV-10 is drifting behind the C130. Oscillating vortex cases are shown in Table 8. There was little discussion of the TKE parameter up to this point because there did not seem to be any correlation with vortex behavior. However, it can now be seen that all these runs are associated with high values of TKE (average value: 1.31). It appears that ambient turbulence was enhancing vortex pair interaction and precipitating the oscillatory motion. Ambient winds were perpendicular to mountains about 300 km upwind, but the atmosphere did not appear to be favorable for mountain wave propagation. Normally these would travel along a discontinuity in the fluid such as an inversion top, but the atmosphere at flight altitude was near neutral and well mixed. Also, there did not seem to be much difference in oscillation wave length from cross wind to head-tail wind orientation as one would expect for a mountain wave. The vertical motion measured from the OV-10 was higher and changed significantly during the course of the runs. There could be more organized vertical motion fields in the atmosphere caused by the turbulent overturning associated with strong cold air advection at flight altitudes. Note that in Flight 556 run 26, some of these oscillations reached altitudes of 150 meters above the generation height. The low points in the vertical sinusoids were 100 meters below C130 flight altitude. The degree of hazard has not yet been determined. The C130 maintained a very steady altitude during these flights.

Vortices remained at or below generation height for all the runs of Flight 557 despite the vertical oscillations. The increased atmospheric stability may have played a role different from buoyancy effects on that day. Increased stability above flight altitude and reduced cold air advection below may have suppressed larger scale vertical motion than might have been active on the previous day.

## 7. Conclusions

Aircraft wakes produced in level flight well above the ground have been shown in several cases to remain near the altitude of their generation and to rise above their generated altitude in a few cases. This is in sharp contrast to wake vortex training material available to the aviation community which depicts wakes descending 500 to 900 feet below their generation altitude. On one occasion the OV-10 was penetrating vortices confirmed by GPS altitude to be above the C130 generation altitude by as much as 150 m. These large excursions were associated with vertical oscillations in the vortex pair most likely triggered by atmospheric turbulence and instability. Turbulence, as measured by the TKE parameter, and neutral stability were highly correlated to the early occurrence of these oscillations. The one documented case (Flight 552, run 9) with no oscillations and where the vortex was above the C130, occurred near the top of an inversion where both buoyancy and wind shear may have played a role. However, the wind shear could not be resolved to a scale sufficient to allow correlation.

## References

1. Hinton, D.A., "Aircraft Vortex Spacing System (AVOSS) Conceptual Design," NASA Tech Memo No 110184, Aug, 1995.
2. Hay, George C. and Robert H. Passman, Wake Turbulence Training Aid, US Department of Transportation, Volpe National Transportation Systems Center, Cambridge, MA, DOT-VNTSC-FAA-95-4, Apr, 1995, page 2.14.
3. Aeronautical Information Manual, US Department of Transportation, Federal Aviation Administration, Nov. 9, 1995, page 7-3-2.
4. Tombach, I., "Observations of Atmospheric Effects on Vortex Wake Behavior," J. Aircraft, Vol 10, 1973, pp. 641-647.
5. Sarpkaya, T., "Trailing Vortices in Homogeneous and Density-Stratified Media," J. Fluid Mech., Vol 136, 1983, pp. 85-109.
6. Greene, G. C., "An Approximate Model of Vortex Decay in the Atmosphere," J. Aircraft, Vol 23, 1986, pp. 566-573.
7. Proctor, F. H., D. A. Hinton, J. Han, D.G. Schowalter, and Y. L. Lin., "Two Dimensional Wake Vortex Simulations in the Atmosphere: Preliminary Sensitivity Studies," AIAA 97-0056, Jan 1997.
8. Higgins, Harry C. "The Thermal Index," Soaring Magazine, Vol. 27, No. 1, 1963, pp. 8-11.
9. Koch, Steven E. et. al., "A Mesoscale Gravity-Wave Event during CCOPE, Part IV: Stability Analysis and Doppler-derived Wave Vertical Structure," Monthly Weather Review, Vol 121, Sep 1993, pp. 2483-2510.
10. Sarpkaya, T. and J. J. Daly, "Effect of Ambient Turbulence on Trailing Vortices," J. Aircraft, Vol. 24, No. 6, Jun 1987, pp. 399-404.
11. Hallock, J. N., "Aircraft Wake Vortices: An Assessment of the Current Situation," DOT-FAA-RD-90-29, Jan, 1991, US Department of Transportation, John A. Volpe National Transportation Systems Center, Cambridge, MA.
12. Stuever, Robert A. Eric C. Stewart, and Robert A. Rivers, "Overview of the Preparation and Use of an OV-10 Aircraft for Wake Vortex Hazards Flight Experiments," AIAA 95-3935, Sep 1995.

Table 1. Flight Summary

<b>Flight # &amp; Date</b>	<b>Time (GMT)</b>	<b># Wake Encounters</b>	<b>Altitude (m)</b>	<b>Synoptic Weather</b>	<b>Wake Behavior</b>
551 19 Oct	1243-1532	4	1550	Clear; High Pressure; Stable; Inv.1100-1400 m	Descends then steady
552 19 Oct	1805-2013	6	1550 <b>1150</b> 800	Sctd Cu; High Pressure; Stable; Inv. 1000-1200 m	Descends then steady to rise
553 26 Oct	1043-1326	5	<b>2200</b> 1600	Clear to Sctd Cu; High Pressure; Haze; Stable; Inv. 1700-2300 m	Steady to slow sink; some rise
555 6 Nov	1608-1857	5	1600 1450	Clear; Cold High Pressure; Weak Inv. 1050-1200	Slow sink
556 8 Nov	1441-1630	9	900	Sctd-Brkn Cu; strong cold advection; neutral; windy; turbc	Large oscillation; some above C130
557 9 Nov	1647-1903	4	1100	Sctd Cu; High Pressure; Neutral to Sable; Inv 2000-2100; 2500- 2600	Large oscillations; all below C130

Table 2. Data Available

<b>Flight-Date</b>	<b>C130 DGPS</b>	<b>OV-10 DGPS</b>	<b>OV-10 GPS &amp; PA</b>	<b>Tail Camera</b>
551-Oct 19	Yes	No	Yes	Yes
552-Oct 19	Yes	No	Yes	No
553-Oct26	No	No	Yes	Yes
555-Nov 6	No	Yes	Yes	No
556-Nov 8	Yes	Yes	Yes	Yes
557-Nov 9	Yes	Yes	Yes	Yes

Table 3. OV-10 Parameters

<b>Aircraft Parameters f(time)</b>	<b>Met Parameters f(time)</b>
X, Y, Z	U,V,W wind
Heading	Direction/Speed
True Air Speed	Temperature
Pitch, roll, yaw and deviations	Pressure-Altitude
	Dew Point

Table 4. Other Meteorological Data Available

<b>Flight date</b>	<b>Routine and Special Upper-Air Times</b>	<b>Surface and Upper-Air</b>
Oct 19 AM	1200, 1400 GMT	1200Z Surface, 850 Hectopascal
Oct 19 PM	1750, 2046 GMT	1200Z Surface, 850 Hectopascal
Oct 26	1131, 1200 GMT	1200Z Surface, 850 Hectopascal
Nov 6	1200, 1730 GMT	1200Z Surface, 850 Hectopascal
Nov 8	1200, 1600 GMT	1200Z Surface, 850 Hectopascal
Nov 9	1200, 1843 GMT	1200Z Surface, 850 Hectopascal

Table 5. Data Summary for Rising Vortex Research

Flight No.	Date	Run No.	Abeam		Penetration		Nom Flt Lvl	Flt Level	IAS	Heading	Orientation	Wake Character	TKE	OV-10	C130
			Beg. Time	End Time	Beg. Time	End Time								Mean Wind	Mean Wind
			HMS-GMT	HMS-GMT	HMS-GMT	HMS-GMT								deg/m/s	deg/m/s
						Feet	meters	m/s	deg			m <sup>2</sup> /s <sup>2</sup>			
551	19-Oct-95														
		6	132743	133000	133154	134238	5000	1540	60	220	HW	sinking	0.12	230/05	224/03
		10	141645	141818	141821	142100	5000	1575	90	220	HW	slow sink -level	0.213	220/07	200/03
		13	144047	144200	144216	144358	5000	1560	90	310	XW		0.222	210/06	N/A
		14	145100	145359	145405	150000	5000	1560	60	310	XW		0.215	220/07	200/05
													AVG 0.214		
552	19-Oct-95														
		5	183433	183650	183707	184200	5000	1540	95	20	TW	sinking	0.142	195/09	190/03
		6	184956	185200	185310	185650	5000	1530	95	300	XW	slow sink - level	0.222	200/06	190/03
		7	190044	190150	190210	190600	3700	1150	95	120	XW	level	0.17	240/04	240/05
		8	190758	190900	190957	191200	3300	1025	95	310	XW	slow sink-level	0.083	225/02	240/05
		9	191735	191900	191910	192250	3300	1025	95	50	TW	sink-rise-sink	0.187	200/04	N/A
		10	192808	192940	192949	193350	2500	775	95	220	HW	slow sink	0.356	200/02	220/05
													AVG 0.249		
553	26-Oct-95														
		8	115324	115530	115550	115750	5200	1600	65	290	HW	*slow sink	0.156	315/06	300/03
		9	120725	120900	120912	121322	5200	1650	100	100	TW	*steady	0.209	280/5.5	305/07
		11	123420	123530	123549	123919	7000	2225	100	80	XW	*slow sink	0.041	255/12	260/16
		12	124600	124734	124736	125007	7000	2225	100	170	XW	*slow sink-level	0.348	260/11	260/10
		13	125925	130115	130133	130400	7000	2225	100	350	XW	*steady-rise	0.115	260/11.5	250/10
													AVG 0.136		
555	6-Nov														
		2	164315	164420	164423	164800	5000	1450	70	360	XW	*slow sink	0.866	270/02	270/05
		3	165540	165730	165810	165940	5000	1450	70	90	TW	*sink	0.176	270/04	270/03
		4	170630	170730	170755	171355	5000	1450	100	270	HW	*sink	0.743	300/03	270/03
		5	173500	173600	173605	173750	5000	1600	70	350	XW	*slow sink	0.386	230/2.5	270/03
		6	175122	175330	175520	175834	5000	1575	70	70	TW	*sink-rise	0.386	260/04	270/03
													AVG 0.626		
556	8-Nov-95														
		22	153450	153550	153650	154317	3000	900	70	300	HW	large oscillations	0.774	308/12	300/08
		23	154743	154918	154925	155335	3000	900	70	120	TW	large oscillations	1.2	290/10	290/12
		24	155650	155750	155755	155953	3000	900	100	300	HW	large oscillations	2.16	300/10	300/09
		25	160750	160844	160900	161316	3000	900	100	120	TW	large oscillations	0.97	290/11	300/13
		26	162145	162245	162255	162750	3000	900	100	210	XW	large oscillations	1.27	300/10	300/10
		27	163230	163323	163330	163650	3000	900	100	30	XW	large oscillations	2.86	300/10	281/11
		28	165213	165320	165330	165755	3000	900	100	210	XW	large oscillations	0.574	312/15	300/11
													AVG 1.40		
557	9-Nov-95														
		22	174103	174200	174245	174603	3800	1100	70	145	TW	large oscillations	1.29	300/10	315/08
		23	174925	175040	175045	175300	3800	1100	70	325	HW	large oscillations	0.873	325/07	300/10
		24	175730	175843	175847	180055	3800	1100	70	65	XW	large oscillations	0.956	300/08	305/20
		25	180642	180725	180732	181019	3800	1100	70	245	XW	large oscillations	1.47	320/10	320/08
													AVG 1.38		

\* C130 altitude was not available and was assumed constant

Table 5. (continued)

Mean Temp	Pot Temp	Mean Dew Point	Mean W	DTh/DZ	DDir/DZ	DS/DZ	B-V	Crosswind Shr	Inversion bse.	Inversion top	Strength
C	K	C	m/s	degK/100m	deg/100m	m/s/100m	per sec	m/s/100m	meters	meters	deg/100m
									1100	1200	2
11.2	297.9	-27.3	0.5	0.7	20	1	0.0151749	1			
11	298	-10	0.5	1	20	1	0.0181345	1			
10.6	298	-7	0.5	1	20	1	0.0181345	0.5			
10.5	298	-6	0.5	1	20	1	0.0181345	0.5			
									900	1100	2
11.3	298	1	0.5	0.5	1	0.3	0.012823	0.1			
11	298	4	0.5	0.5	1	0.3	0.012823	0.3			
13.4	295.5	-21	0.5	0.8	20	0.3	0.0162884	1			
13.2	295	-10	0.2	1.1	20	0.3	0.0191161	1			
13.5	295	-10	1	1.1	20	0.3	0.0191161	1			
13.5	291	3	0.2	0.5	2	0.3	0.0129763	0.1			
									1700	2300	2.4
3.4	292	-0.5	0.6	0.4	7	0.3	0.0115865	1.5			
4	292	-2	0.4	0.6	10	0.3	0.0141905	1.5			
6	301	-15	0.4	2.4	15	1.3	0.0279534	0.3			
6	301	-13.6	0.5	2.4	5	13	0.0279534	0.3			
6.5	301	-15	0.2	2.4	5	1.3	0.0279534	0.3			
									1100	1300	2
-1.5	285	-7.8	0.5	0.4	12	0.8	0.0117279	0.4			
-1.5	285	-8.3	0.5	0.4	12	0.8	0.0117279	0			
-1	285	-8.6	0.5	0.4	12	0.8	0.0117279	0			
-2	289	-8.8	0.5	0.4	7	0.8	0.0116465	0.4			
-2	288	-9.3	0.5	0.4	8	0.8	0.0116667	0			
									1300	1500	1
1.9	285	-2	1	0	1	0.5	0	0			
1.5	285	-1	1	0	1	0.5	0	0			
1.5	285	-1	1.5	0	1	0.5	0	0			
1.5	285	-1	1	0	1	0.5	0	0			
1.5	285	-1	1.5	0	1	0.5	0	0.5			
1.5	285	-2	2	0	1	0.5	0	0.5			
0.5	285	-2	2	0	1	0.5	0	0.5			
									1280	1500	1
-7	275.5	-8	1	0	1.5	0.5	0	0			
-6.7	275.5	-10	0.8	0	1.5	0.5	0	0.2			
-7	275.5	-10	0.8	0	1.5	0.5	0	1			
-6.8	275.5	-9	0.8	0	1.5	0.5	0	1			

Table 6. Data Summary for Sinking Vortices

Flight No.	Date	Run No.	Abeam		Penetration		Nom Flt Lvl	Flt Level	IAS	Heading	Orientation	Wake Character
			Beg. Time	End Time	Beg. Time	End Time						
			HMS-GMT	HMS-GMT	HMS-GMT	HMS-GMT						
551	19-Oct-95											
		6	132743	133000	133154	134238	5000	1540	60	220	HW	sinking
552	19-Oct-95											
		5	183433	183650	183707	184200	5000	1540	95	20	TW	sink - level
		10	192808	192940	192949	193350	2500	775	95	220	HW	slow sink
553	26-Oct-95											
		8	115324	115530	115550	115750	5200	1600	65	290	HW	*slow sink
555	6-Nov-95											
		3	165540	165730	165810	165940	5000	1450	70	90	TW	*sink
		4	170630	170730	170755	171355	5000	1450	100	270	HW	*sink

\* C130 altitude was not available and was assumed constant

	OV-10	C130									
TKE	Mean Wind	Mean Wind	Mean Temp	Pot Temp	Mean Dew Point	Mean W	DTh/DZ	DDir/DZ	DS/DZ	B-V	Crosswind Shr
m <sup>2</sup> /s <sup>2</sup>	deg/m/s	deg/m/s	C	K	C	m/s	C/100m	deg/100m	m/s/100m	per sec	m/s/100m
N/A	230/05	224/03	11.2	24.9	-27.3	0.5	0.7	20	1	0.015175	1
0.142	195/09	190/03	11.3	25	1	0.5	0.5	1	0.3	0.012823	0.1
0.356	200/02	220/05	13.5	18	3	0.2	0.5	2	0.3	0.012976	0.1
0.156	315/06	300/03	3.4	19	-0.5	0.6	0.4	7	0.3	0.011586	1.5
0.176	270/04	270/03	-1.5	12	-8.3	0.5	0.4	12	0.8	0.011728	0
0.743	300/03	270/03	-1	12	-8.6	0.5	0.4	12	0.8	0.011728	0
AVG 0.315						AVG 0.47	AVG 0.48			AVG 0.01267	

Table 7. Data Summary for Rising Vortices

Flight No.	Date	Run No.	Abeam		Penetration		Nom Flt Lvl Feet	Flt Level meters	IAS m/s	Heading deg	Orientation	Wake Character	TKE m <sup>2</sup> /s <sup>2</sup>	OV-10
			Beg. Time	End Time	Beg. Time	End Time								Mean Wind
			HMS-GMT	HMS-GMT	HMS-GMT	HMS-GMT								deg/m/s
551	19-Oct-95													
		10	141645	141818	141821	142100	5000	1575	90	220	HW	slow sink - level	0.213	220/07
552	19-Oct-95													
		6	184956	185200	185310	185650	5000	1530	95	300	XW	slow sink - level	0.222	200/06
		7	190044	190150	190210	190600	3700	1150	95	120	XW	slow sink-rise	0.17	240/04
		9	191735	191900	191910	192250	3300	1025	95	50	TW	sink-rise-sink	0.187	200/04
553	26-Oct-95													
		13	125925	130115	130133	130400	7000	2225	100	350	XW	*steady-rise	0.115	260/11.5
555	6-Nov-95													
		6	175122	175330	175520	175834	5000	1575	70	70	TW	*sink-rise	0.386	260/04
													AVG 0.216	

\* C130 altitude was not available and was assumed constant

C130												
Mean Wind	Mean Temp	Pot Temp	Mean DewPoint	Mean W	DTh/DZ	DDir/DZ	DS/DZ	B-V	Crosswind Shr	Inversion bse.	Inversion top	Strength
deg/m/s	C	K	C	m/s	C/100m	deg/100m	m/s/100m	per sec	m/s/100m	meters	meters	deg/100m
										1100	1200	2
200/03	11	25	-10	0.5	1	20	1	0.018134	1			
										900	1100	2
190/03	11	25	4	0.5	0.5	1	0.3	0.012823	0.3			
240/05	13.4	22.5	-21	0.5	0.8	20	0.3	0.016288	1			
N/A	13.5	295	-10	1	1.1	20	0.3	0.019116	1			
										1700	2300	2.4
250/10	6.5	28	-15	0.2	2.4	5	1.3	0.027953	0.3			
										1100	1300	2
270/03	-2	15	-9.3	0.5	0.4	8	0.8	0.011667	0			
				AVG 0.533	AVG 1.033			AVG 0.018				

Table 8. Data Summary for Wakes with Large Oscillations

Flight No.	Date	Run No.	Abeam		Penetration		Nom Flt Lvl	Flt Level	IAS	Heading	Orientation	Wake Character	TKE	OV-10
			Beg. Time	End Time	Beg. Time	End Time								Mean Wind
			HMS-GMT	HMS-GMT	HMS-GMT	HMS-GMT								deg/m/s
556	8-Nov-95													
		22	153450	153550	153650	154317	3000	900	70	300	HW	large oscillations	0.774	308/12
		23	154743	154918	154925	155335	3000	900	70	120	TW	large oscillations	1.2	290/10
		24	155650	155750	155755	155953	3000	900	100	300	HW	large oscillations	2.16	300/10
		25	160750	160844	160900	161316	3000	900	100	120	TW	large oscillations	0.97	290/11
		26	162145	162245	162255	162750	3000	900	100	210	XW	large oscillations	1.27	300/10
		27	163230	163323	163330	163650	3000	900	100	30	XW	large oscillations	2.86	300/10
		28	165213	165320	165330	165755	3000	900	100	210	XW	large oscillations	0.574	312/15
557	9-Nov-95													
		22	174103	174200	174245	174603	3800	1100	70	145	TW	large oscillations	1.29	300/10
		23	174925	175040	175045	175300	3800	1100	70	325	HW	large oscillations	0.873	325/07
		24	175730	175843	175847	180055	3800	1100	70	65	XW	large oscillations	0.956	300/08
		25	180642	180725	180732	181019	3800	1100	70	245	XW	large oscillations	1.47	320/10
													AVG 1.31	

C130												
Mean Wind	Mean Temp	Pot Temp	Mean Dew Point	Mean W	DTh/DZ	DDir/DZ	DS/DZ	B-V	Crosswind Shr	Inversion bse.	Inversion top	Strength
deg/m/s	C	K	C	m/s	C/100m	deg/100m	m/s/100m	per sec	m/s/100m	meters	meters	deg/100m
										1300	1500	1
300/08	1.9	12	-2	1	0	1	0.5	0	0			
290/12	1.5	12	-1	1	0	1	0.5	0	0			
300/09	1.5	12	-1	1.5	0	1	0.5	0	0			
300/13	1.5	12	-1	1	0	1	0.5	0	0			
300/10	1.5	12	-1	1.5	0	1	0.5	0	0.5			
281/11	1.5	12	-2	2	0	1	0.5	0	0.5			
300/11	0.5	12	-2	2	0	1	0.5	0	0.5			
										1280	1500	1
315/08	-7	2.5	-8	1	0	1.5	0.5	0	0			
300/10	-6.7	2.5	-10	0.8	0	1.5	0.5	0	0.2			
305/20	-7	2.5	-10	0.8	0	1.5	0.5	0	1			
320/08	-6.8	2.5	-9	0.8	0	1.5	0.5	0	1			
AVG 1.22												

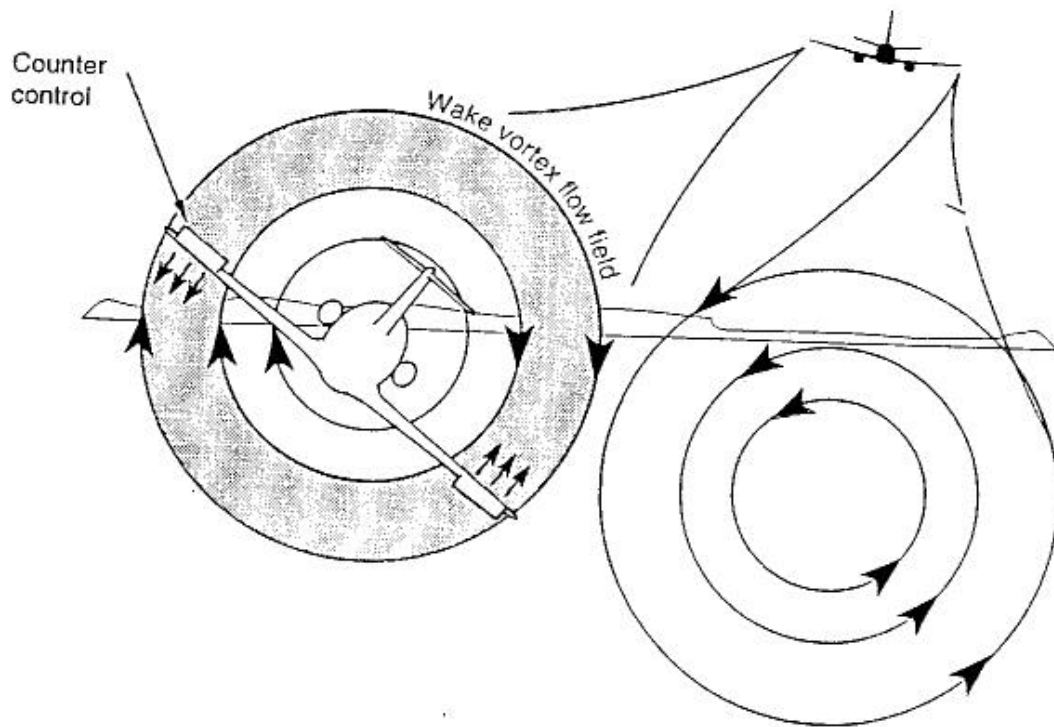


Figure 1. Wake Vortex Flow Field (from ref. 2)

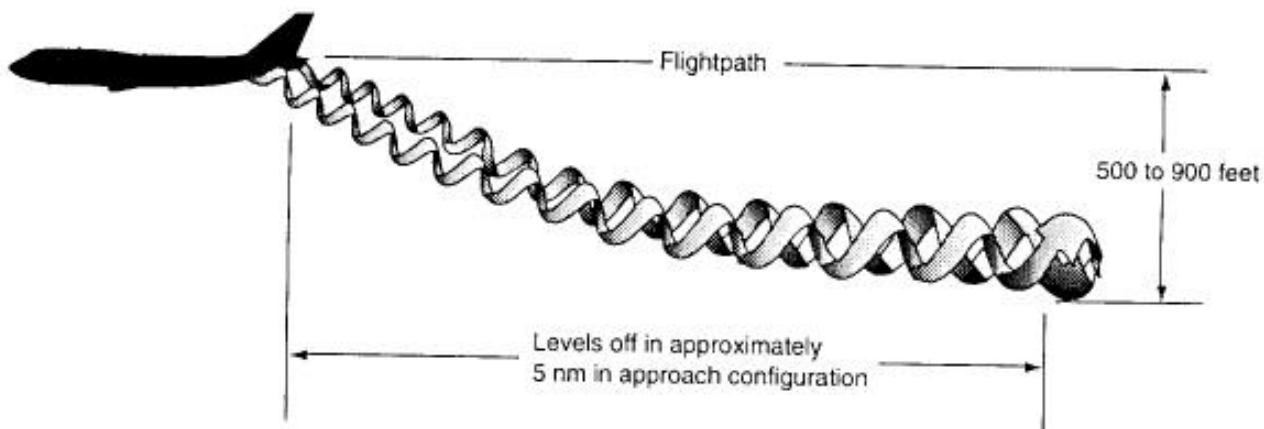


Figure 2. Wake Vortex Descent Rates (from ref. 2)



Figure 3. Video Frame of OV-10 Drifting Behind the C130



Figure 4a. Video Frame of OV-10 Level with the Starboard Vortex



Figure 4b. Video Frame of OV-10 Penetrating Starboard Vortex



Figure 4c. Video Frame of OV-10 Below the Port Vortex

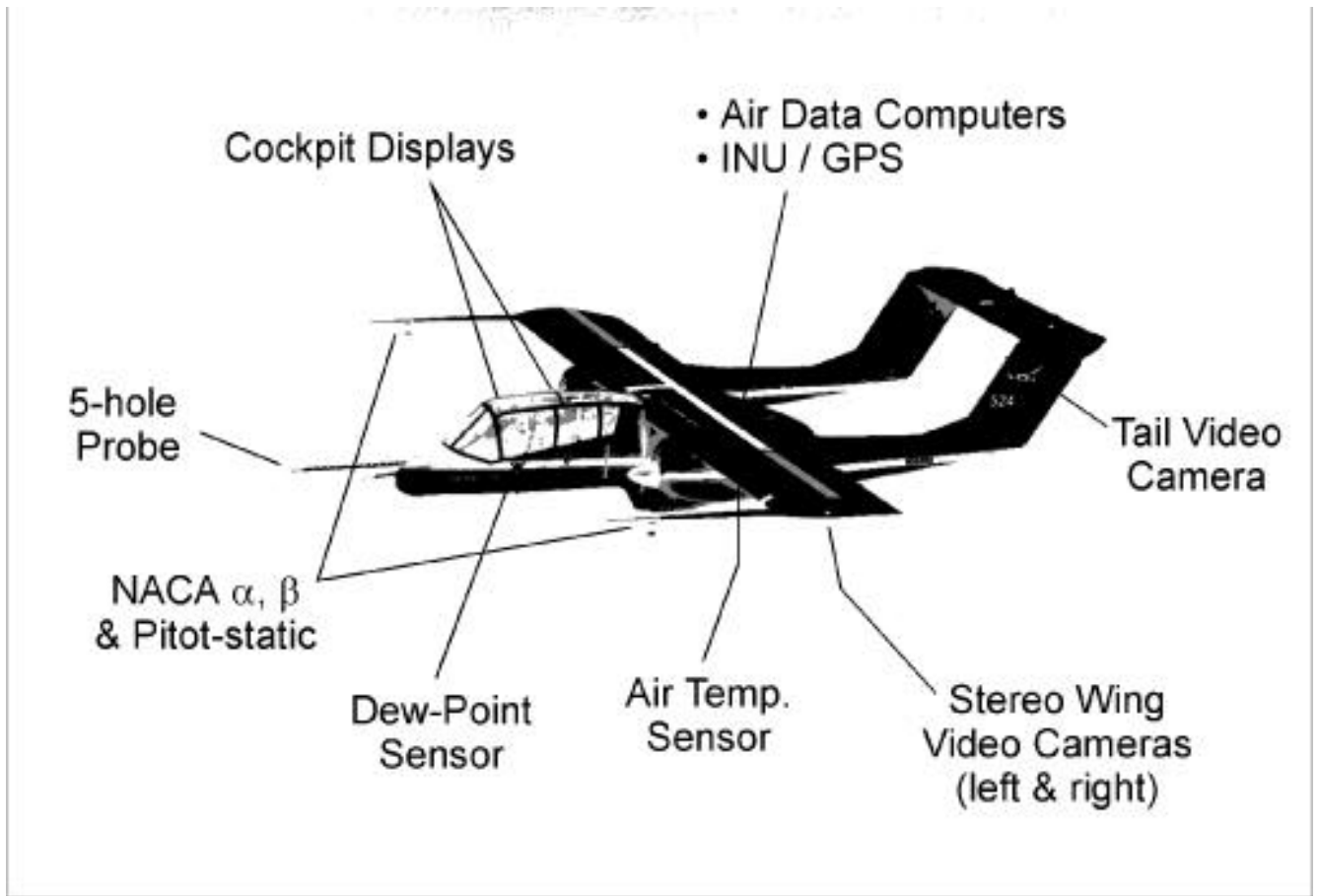


Figure 5. OV-10 Experimental Configuration

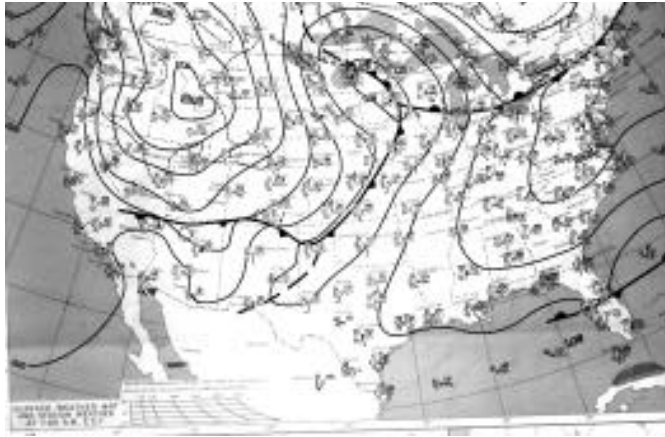


Figure 6a. Surface Weather Map for October 19, 1995, 1200 GMT

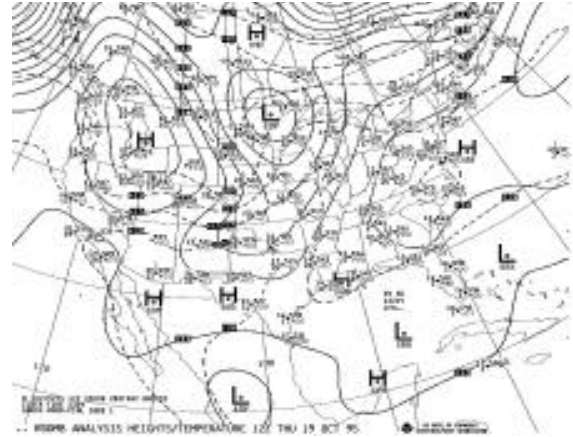


Figure 6b. 850 Hectopascal Weather Map for October 19, 1995, 1200 GMT

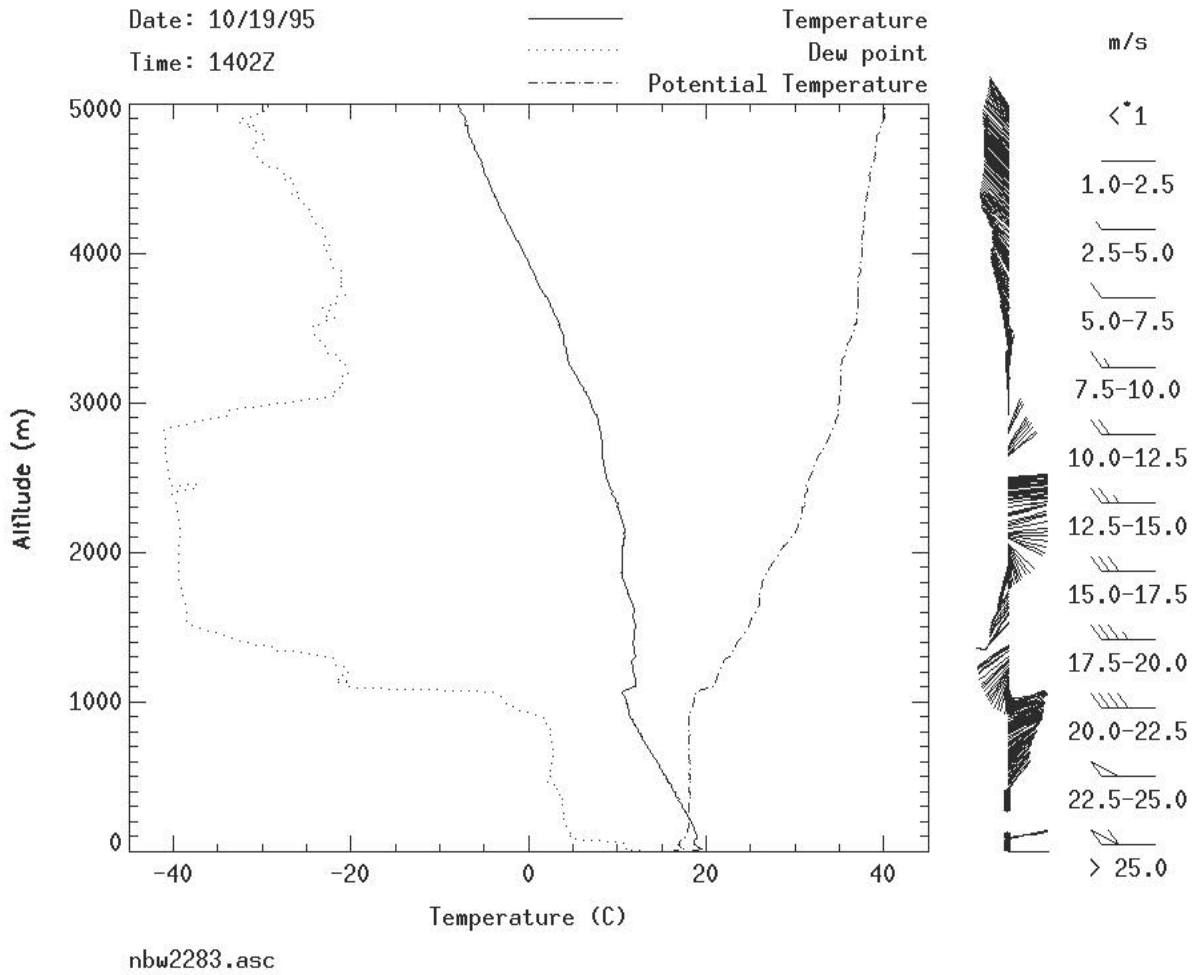


Figure 6c. Balloon Sounding for October 19, 1995, 1400 GMT

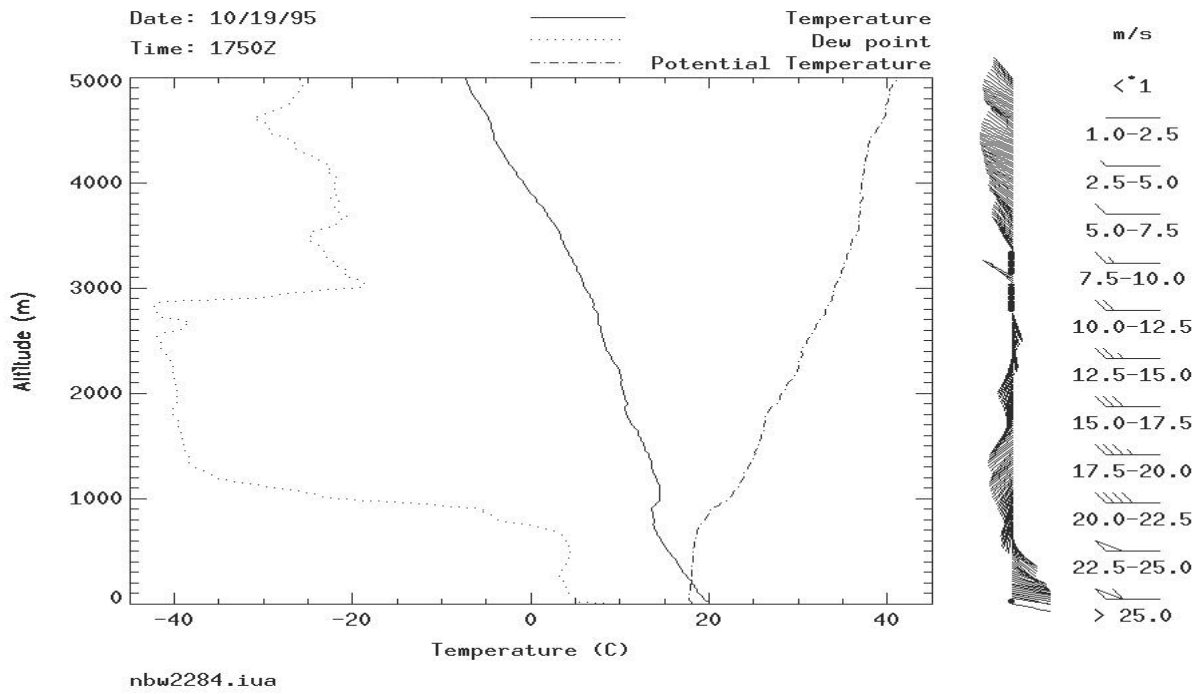


Figure 6d. Balloon Sounding for October 19, 1995, 1750 GMT

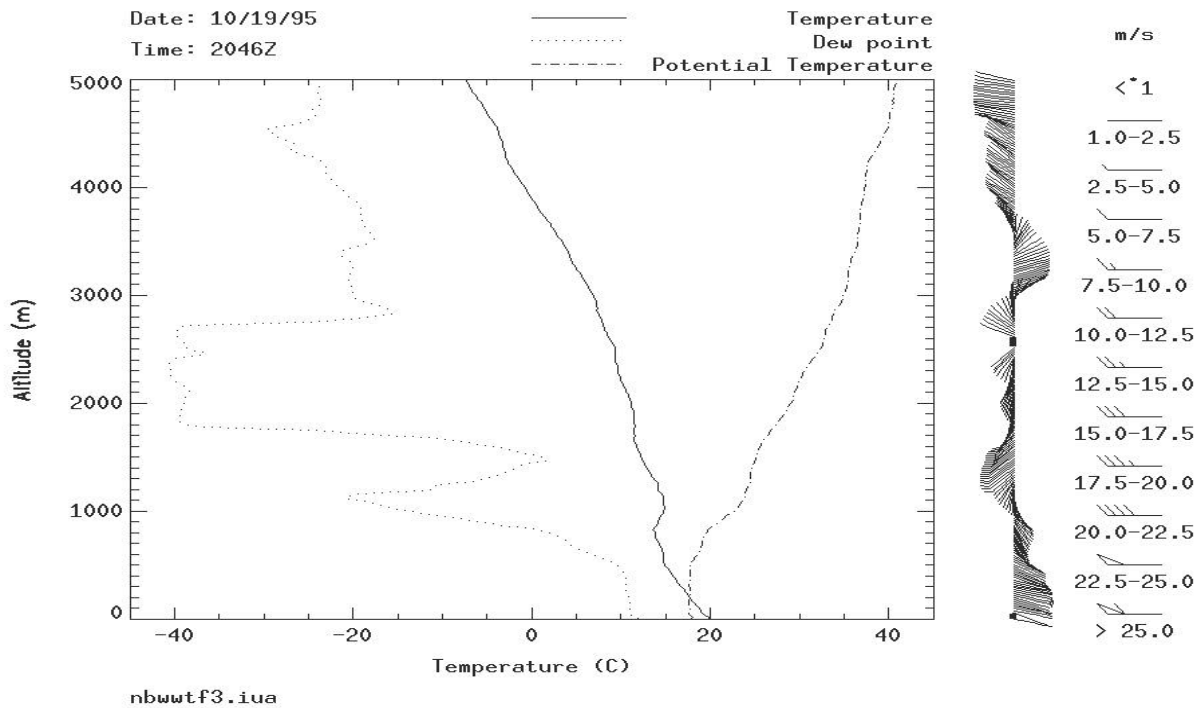


Figure 6e. Balloon Sounding for October 19, 1995, 2046 GMT

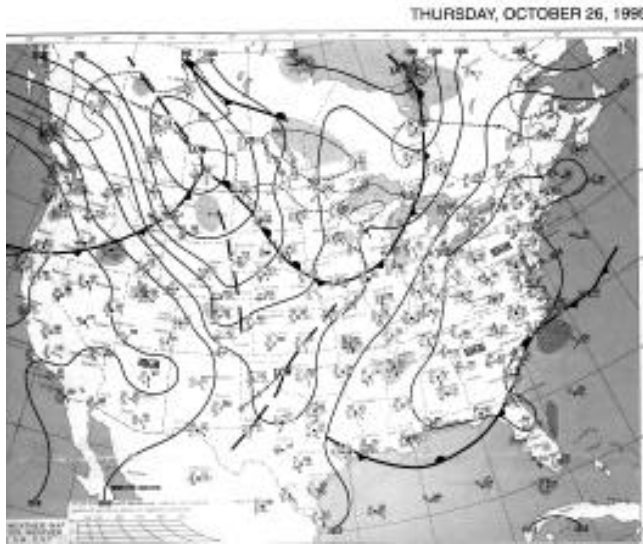


Figure 7a. Surface Weather Map for October 26, 1995, 1200 GMT

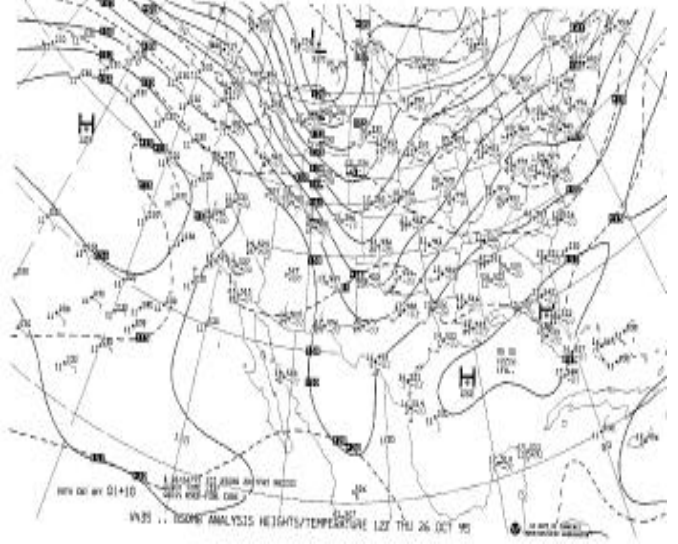


Figure 7b. 850 Hectopascal Weather Map for October 26, 1995, 1200 GMT

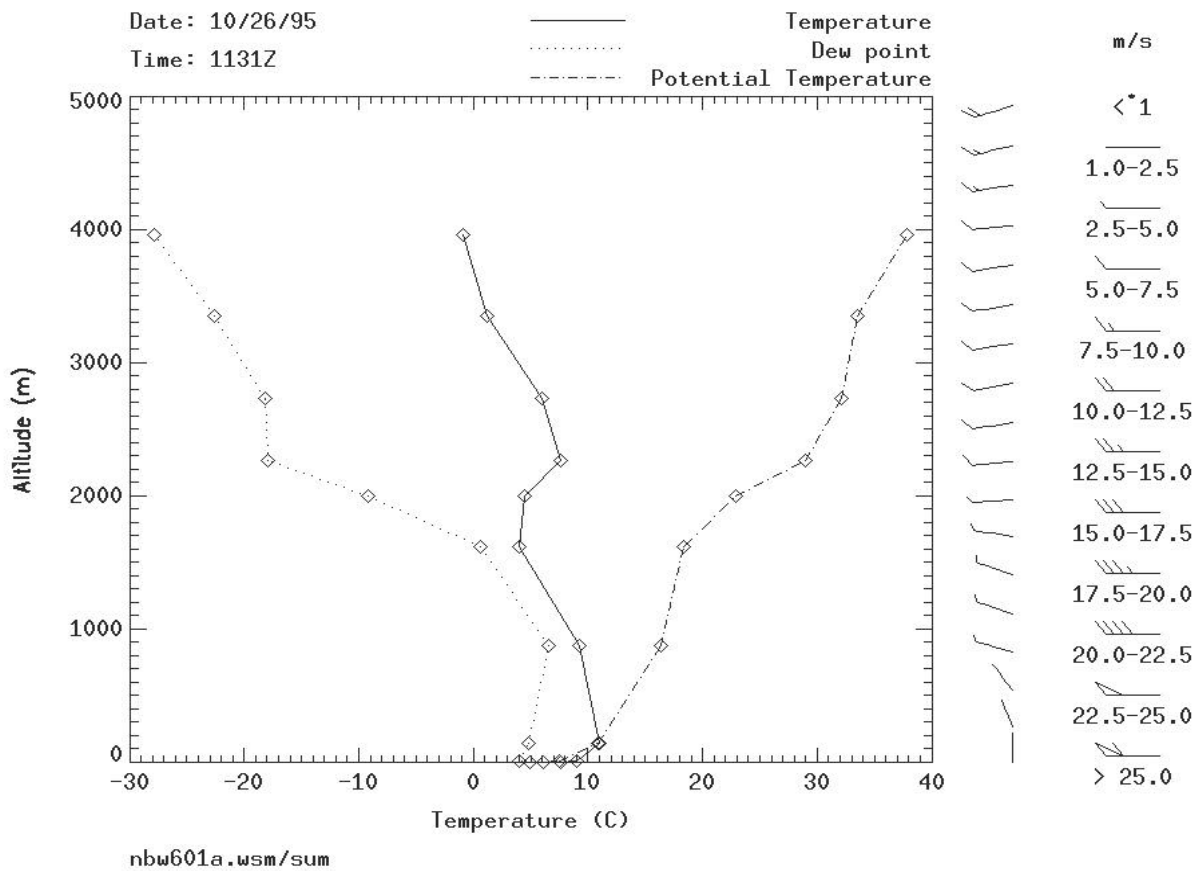


Figure 7c. Balloon Sounding for October 26, 1995, 1131 GMT

MONDAY, NOVEMBER 6, 1995

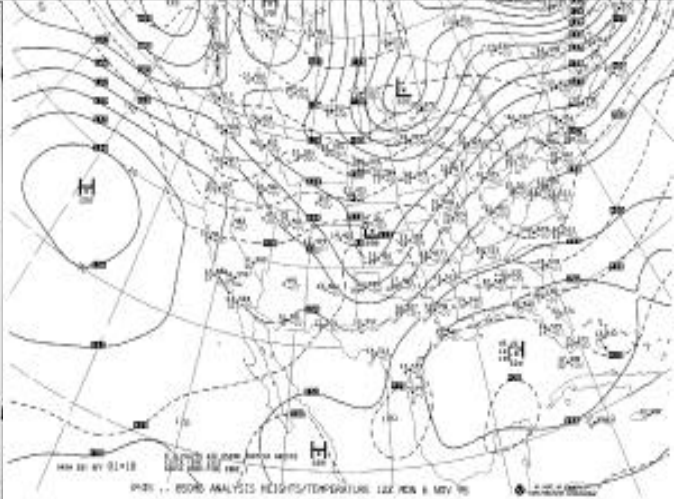
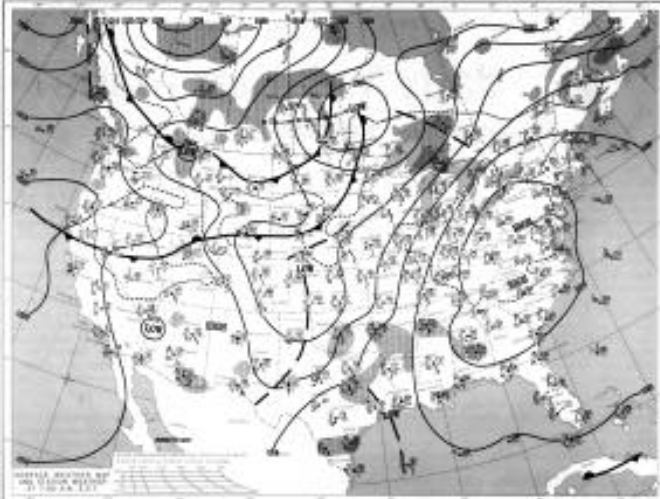


Figure 8a. Surface Weather Map for November 6, 1995, 1200 GMT

Figure 8b. 850 Hectopascal Weather Map for November 6, 1995, 1200 GMT

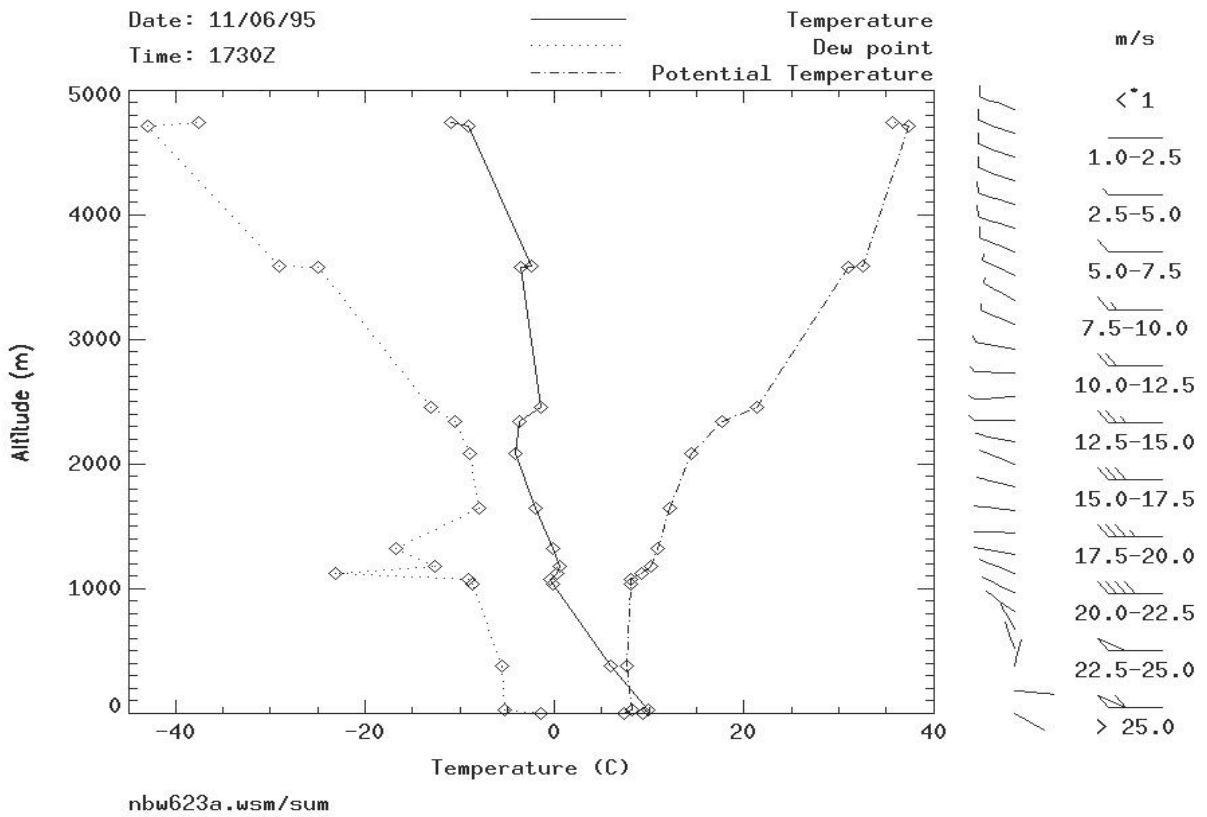


Figure 8c. Balloon Sounding for November 6, 1995, 1730 GMT

WEDNESDAY, NOVEMBER 8, 1995

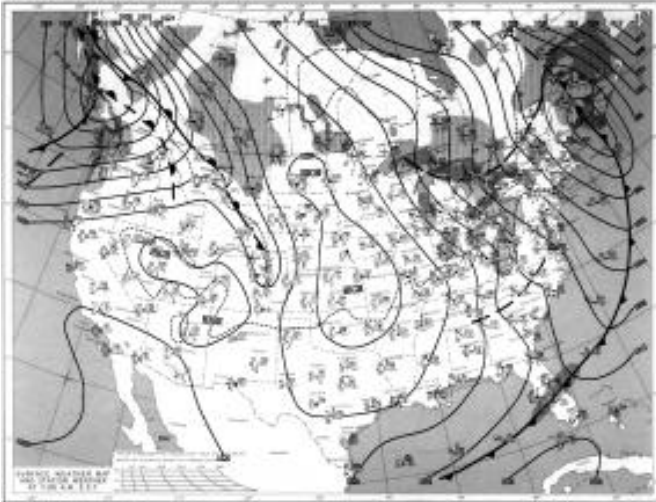


Figure 9a. Surface Weather Map for November 8, 1995, 1200 GMT

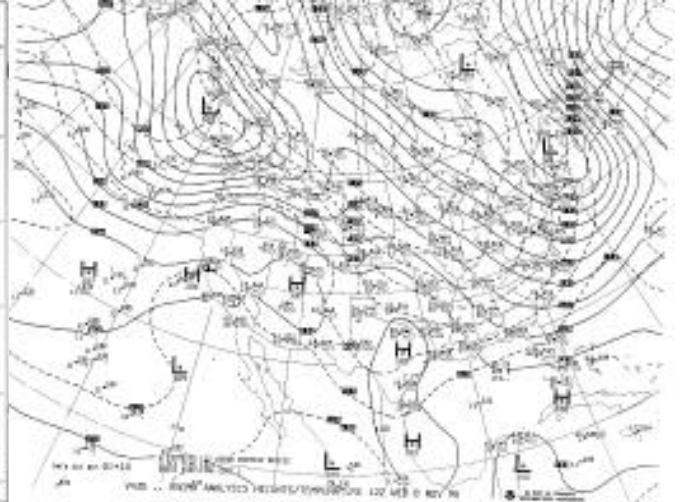


Figure 9b. 850 Hectopascal Weather Map for November 8, 1995, 1200 GMT

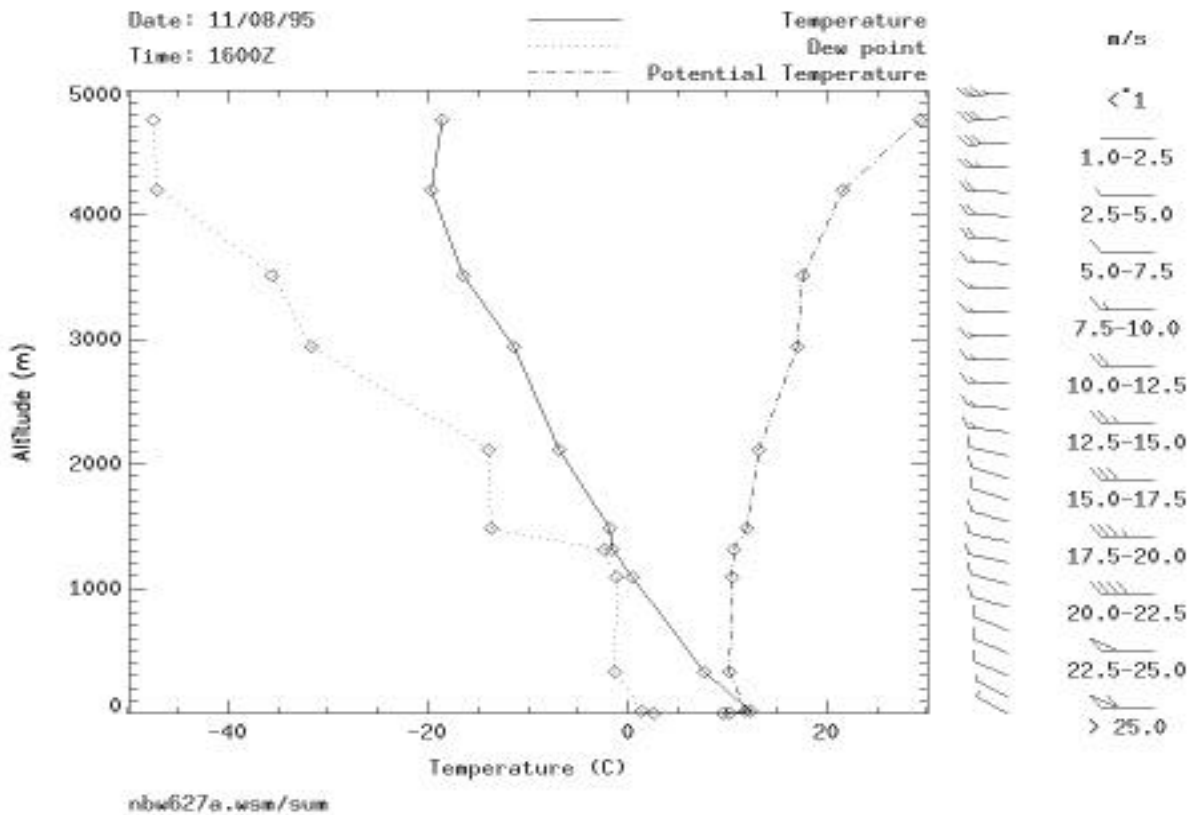


Figure 9c. Balloon Sounding for November 8, 1995, 1600 GMT

THURSDAY, NOVEMBER 9, 1995

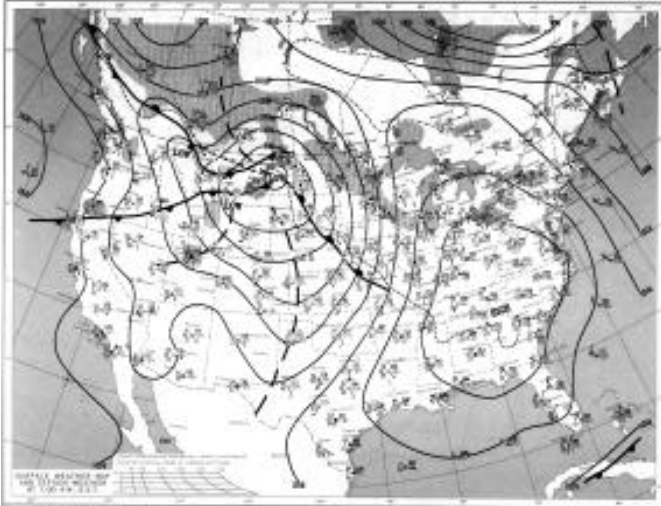


Figure 10a. Surface Weather Map for November 9, 1995, 1200 GMT

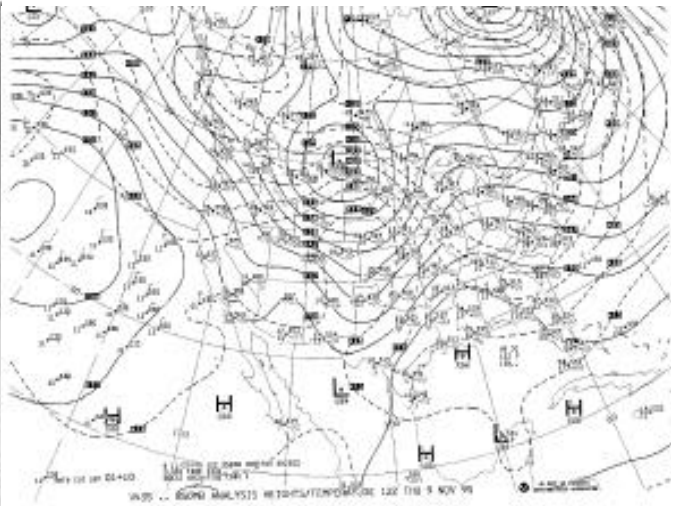


Figure 10b. 850 Hectopascal Weather Map for November 9, 1995, 1200 GMT

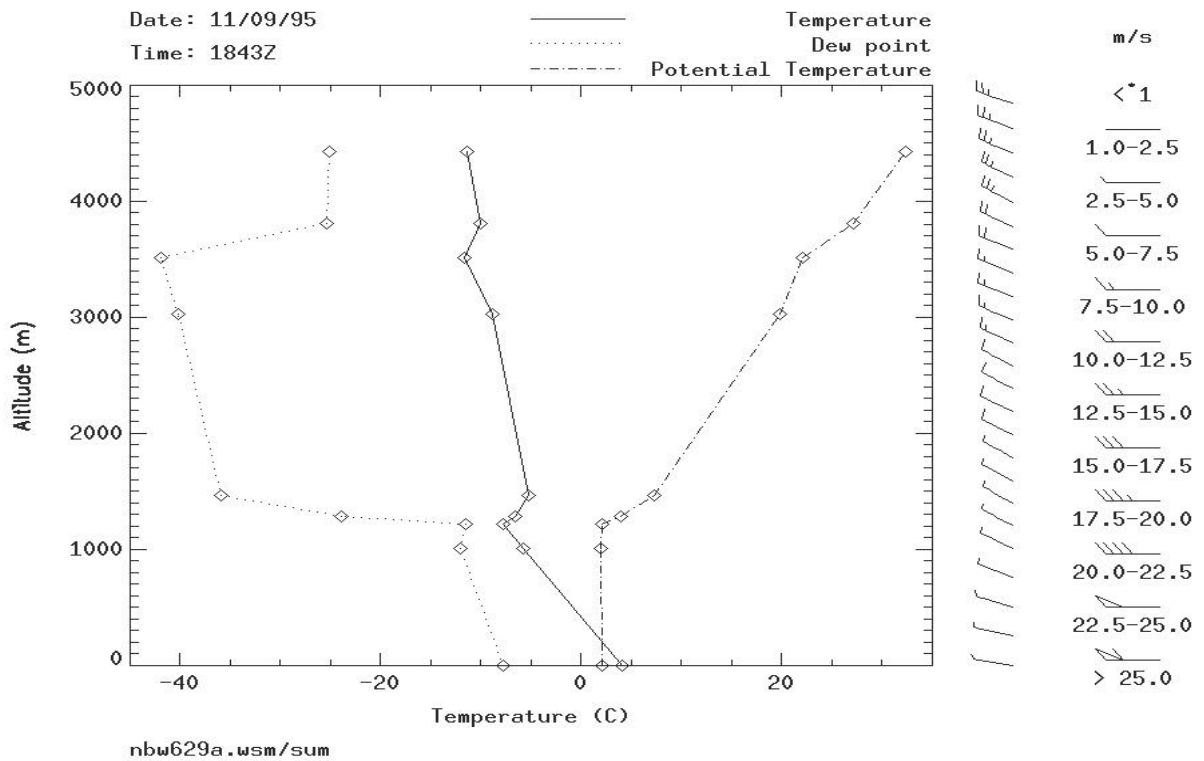


Figure 10c. Balloon Sounding for November 9, 1995, 1843 GMT

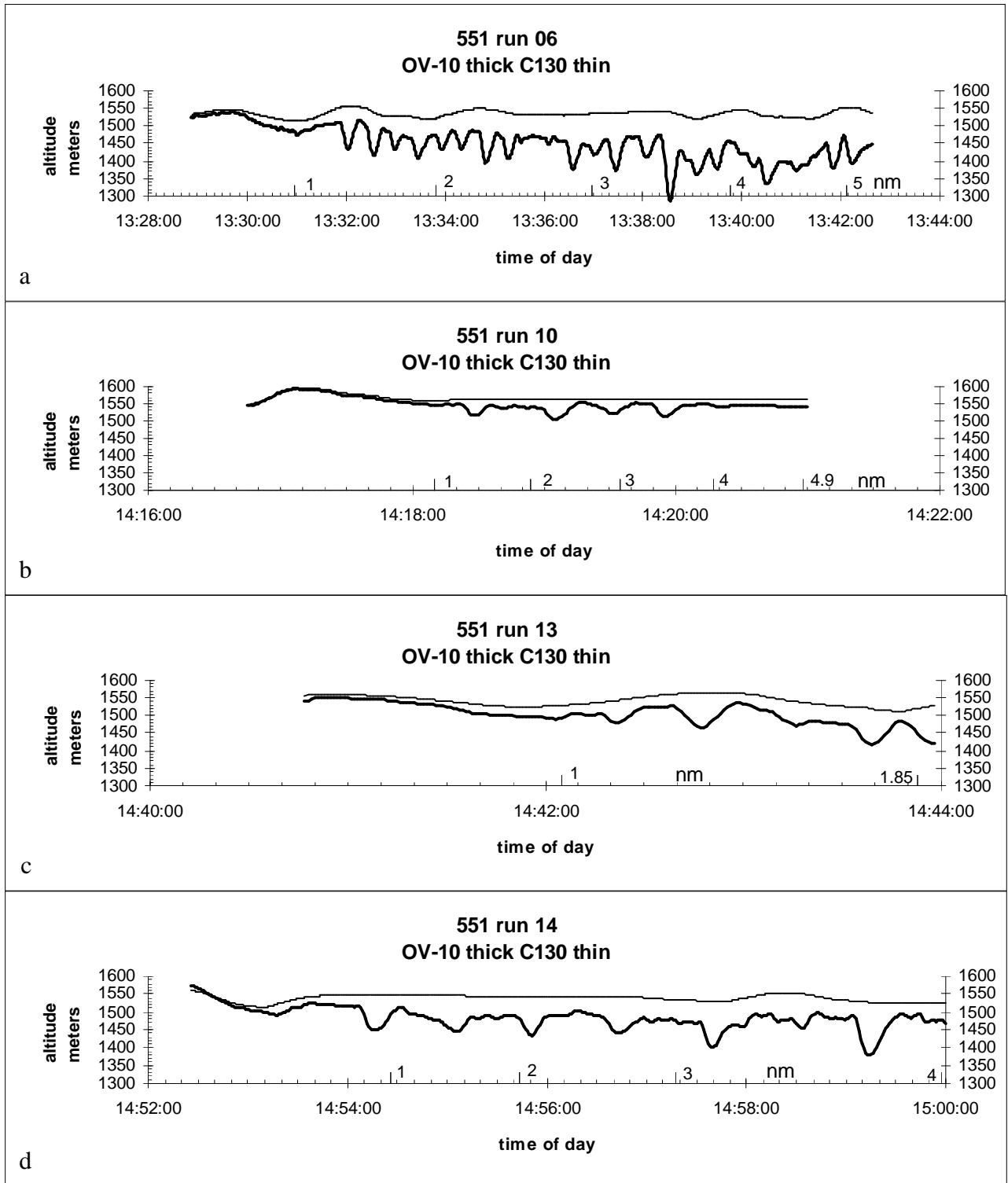


Figure 11. C130 and OV-10 GPS Altitude for Flight 551 at Run Times Shown

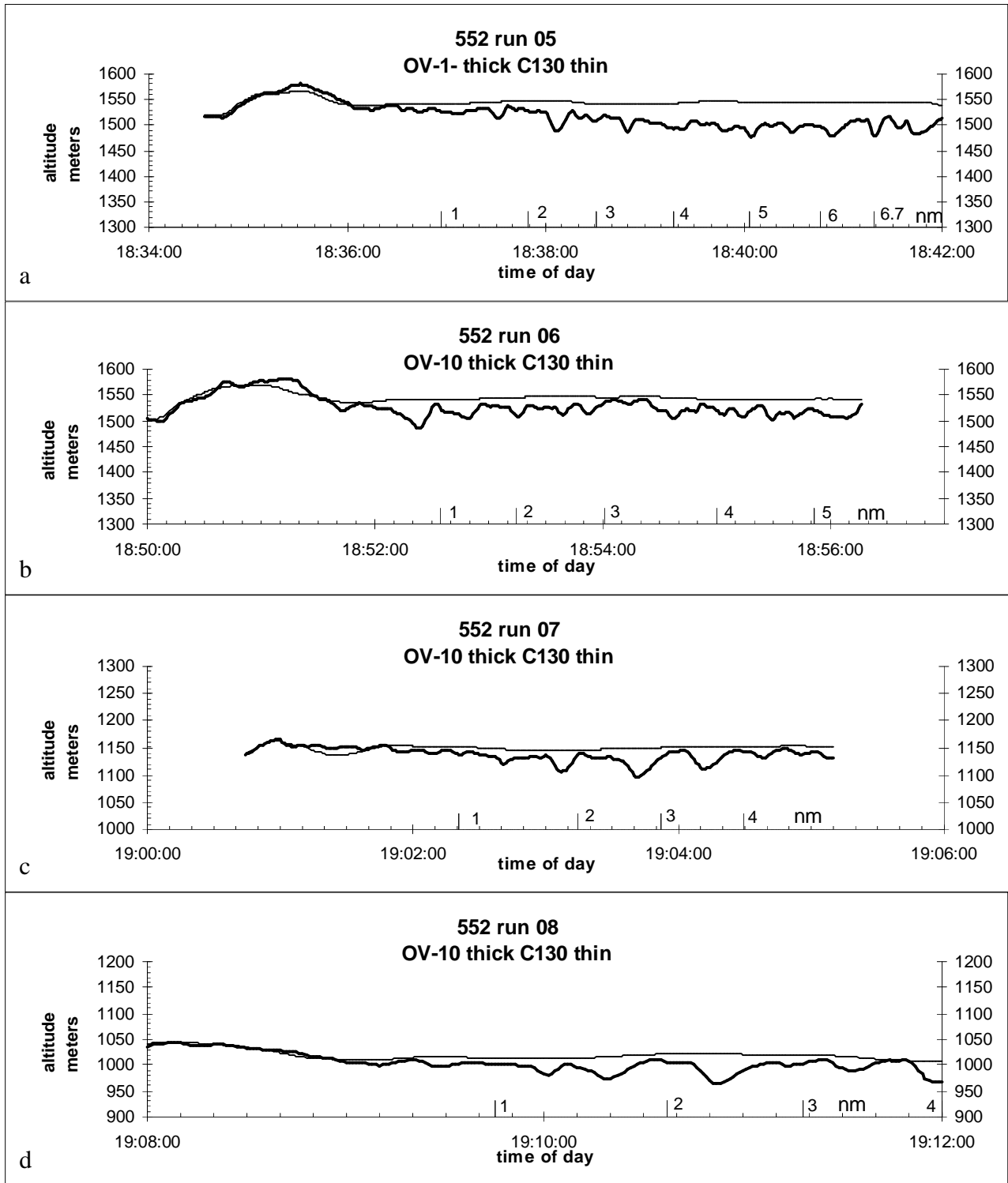


Figure 12. C130 and OV-10 GPS Altitude for Flight 552 at Run Times Shown

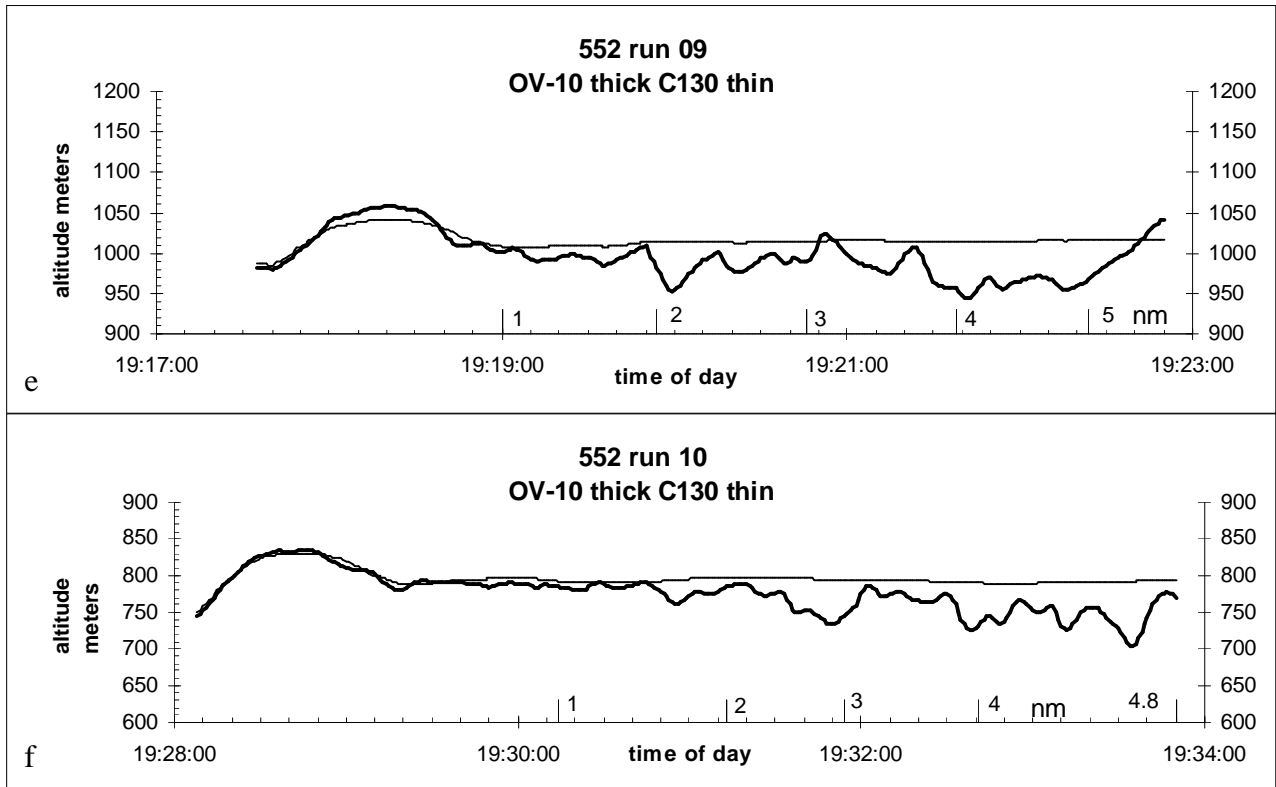


Figure 12. (continued) C130 and OV-10 GPS Altitude for Flight 552 at Run Times Shown

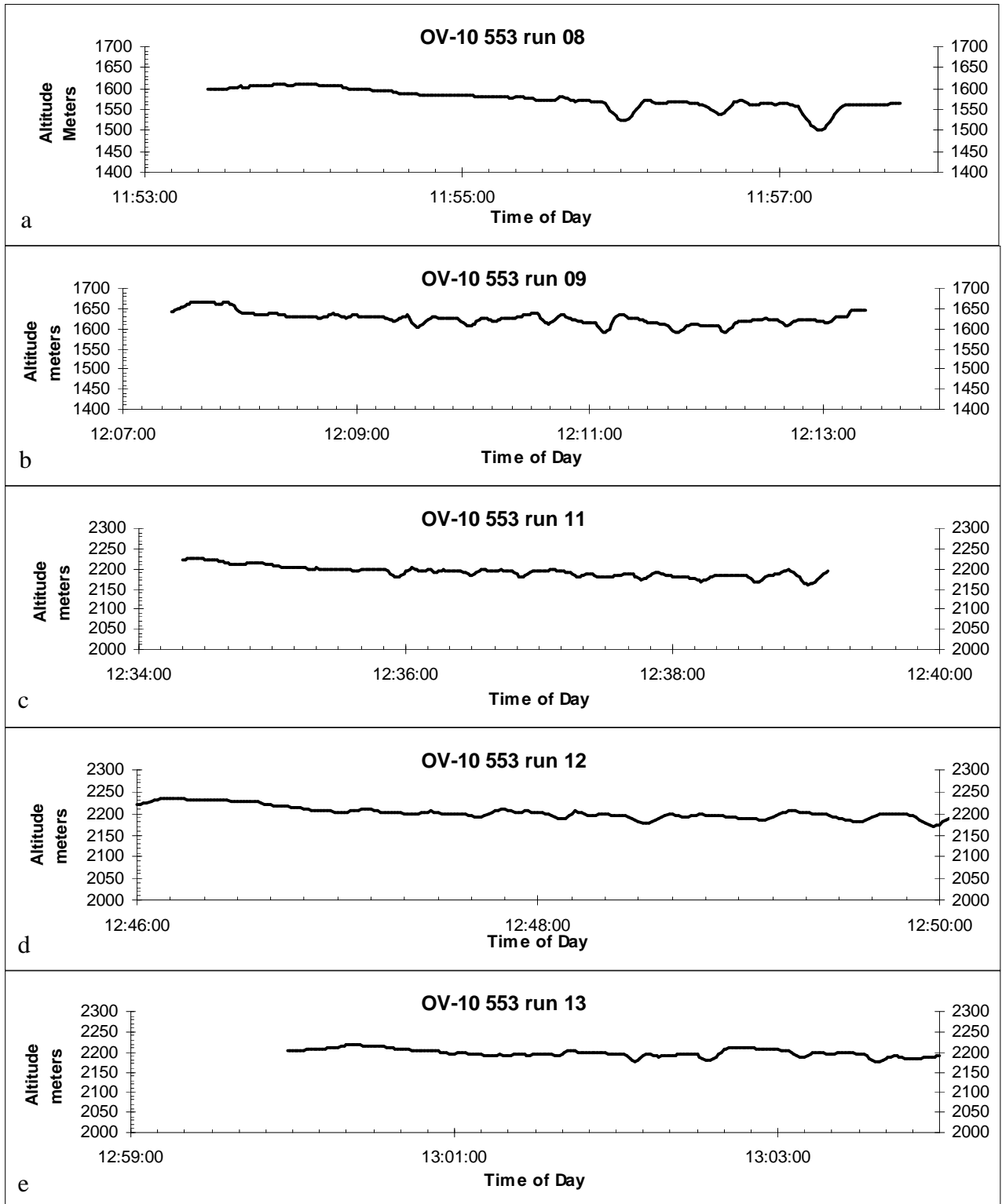


Figure 13. C130 and OV-10 GPS Altitude for Flight 553 at Run Times Shown

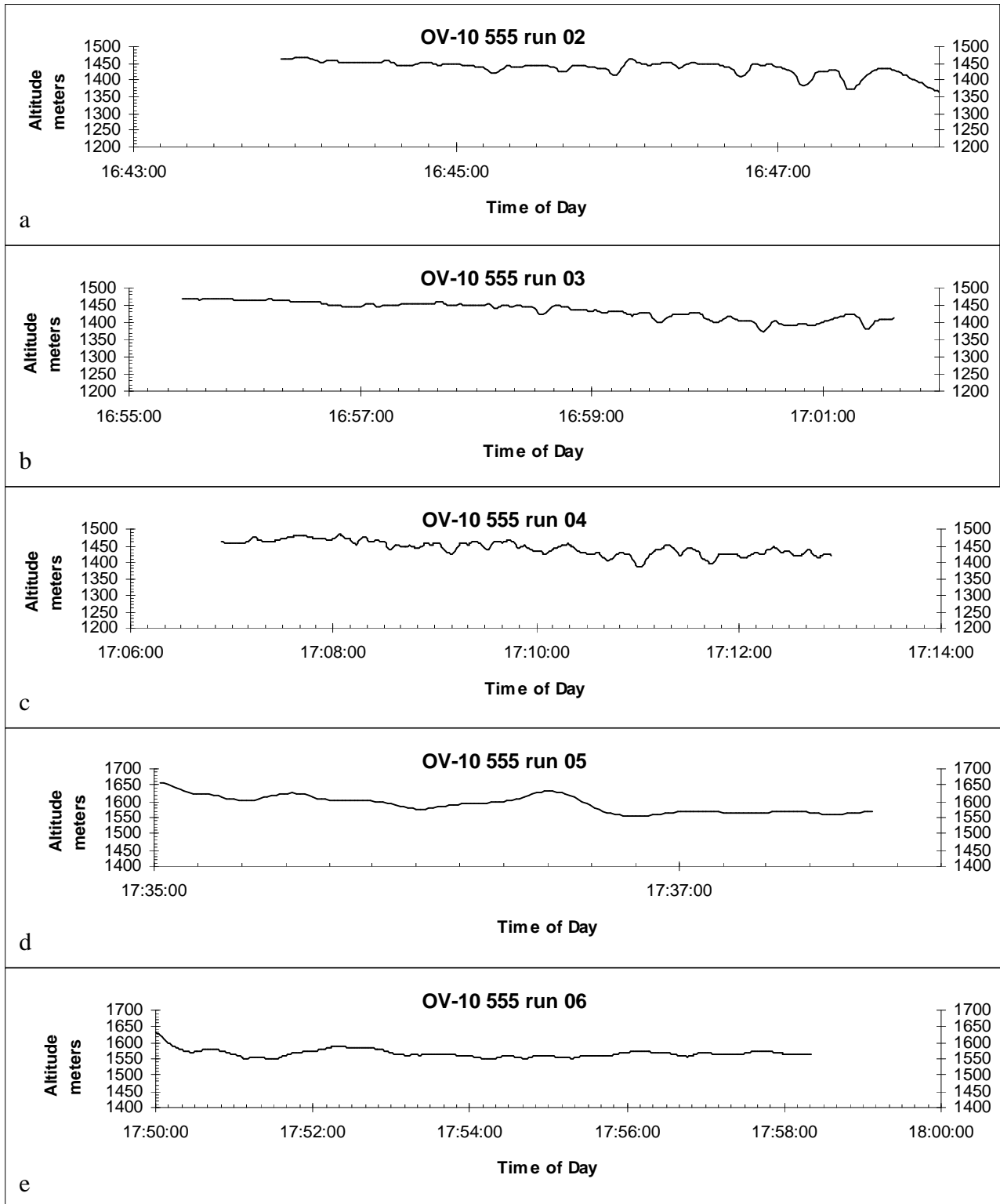


Figure 14. C130 and OV-10 GPS Altitude for Flight 555 at Run Times Shown

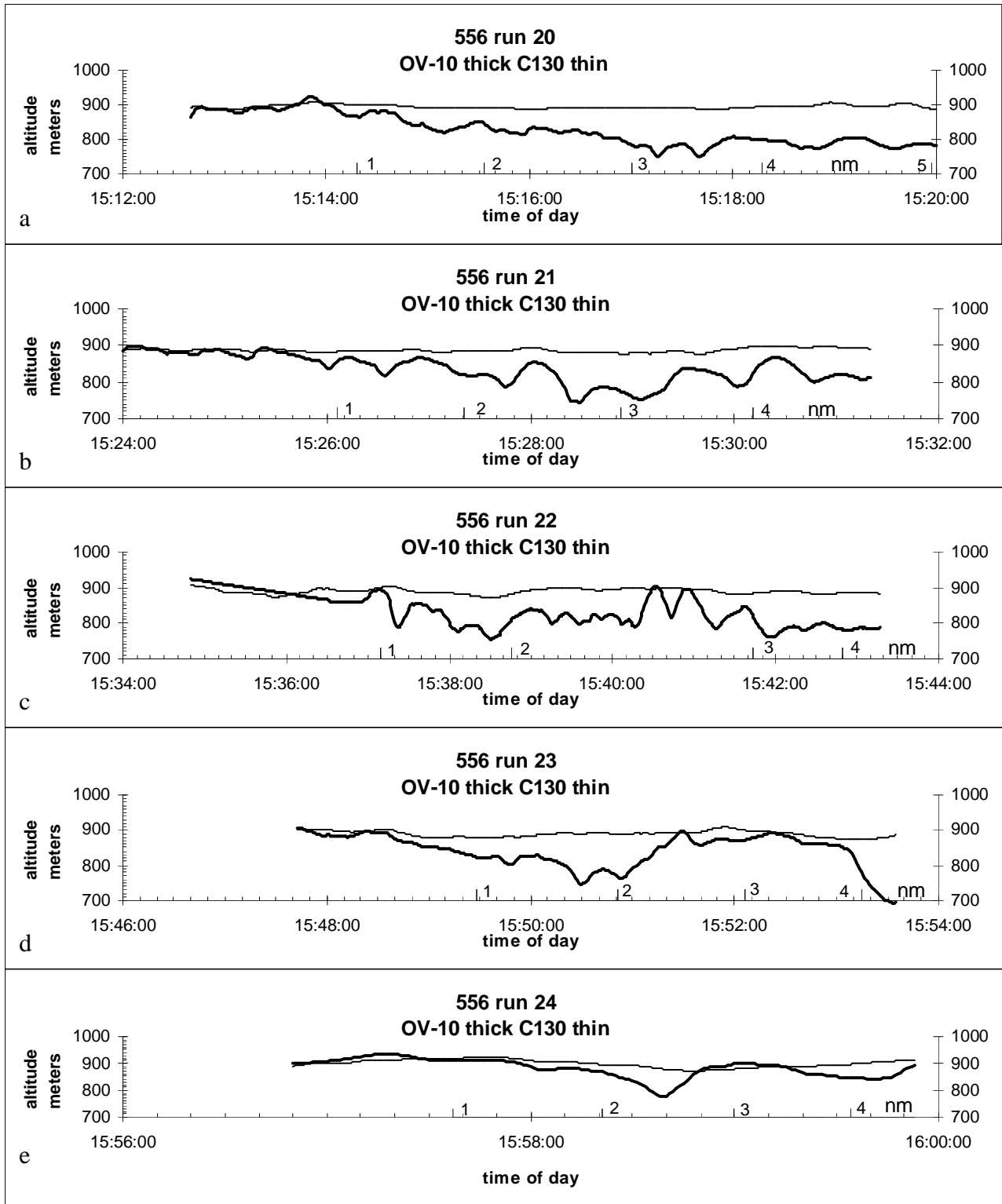


Figure 15. C130 and OV-10 GPS Altitude for Flight 556 at Run Times Shown

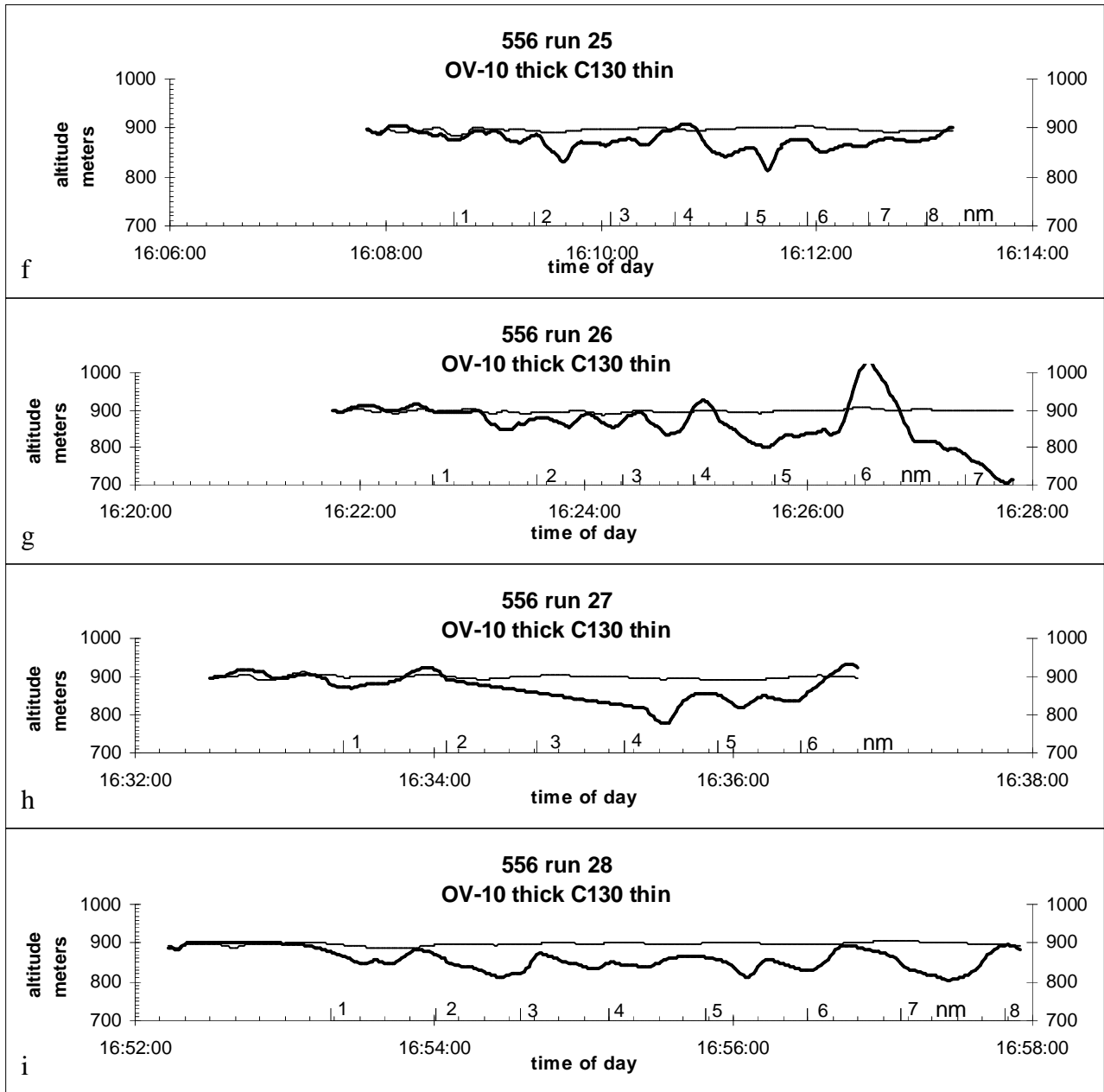


Figure 15. (continued) C130 and OV-10 GPS Altitude for Flight 556 at Run Times Shown

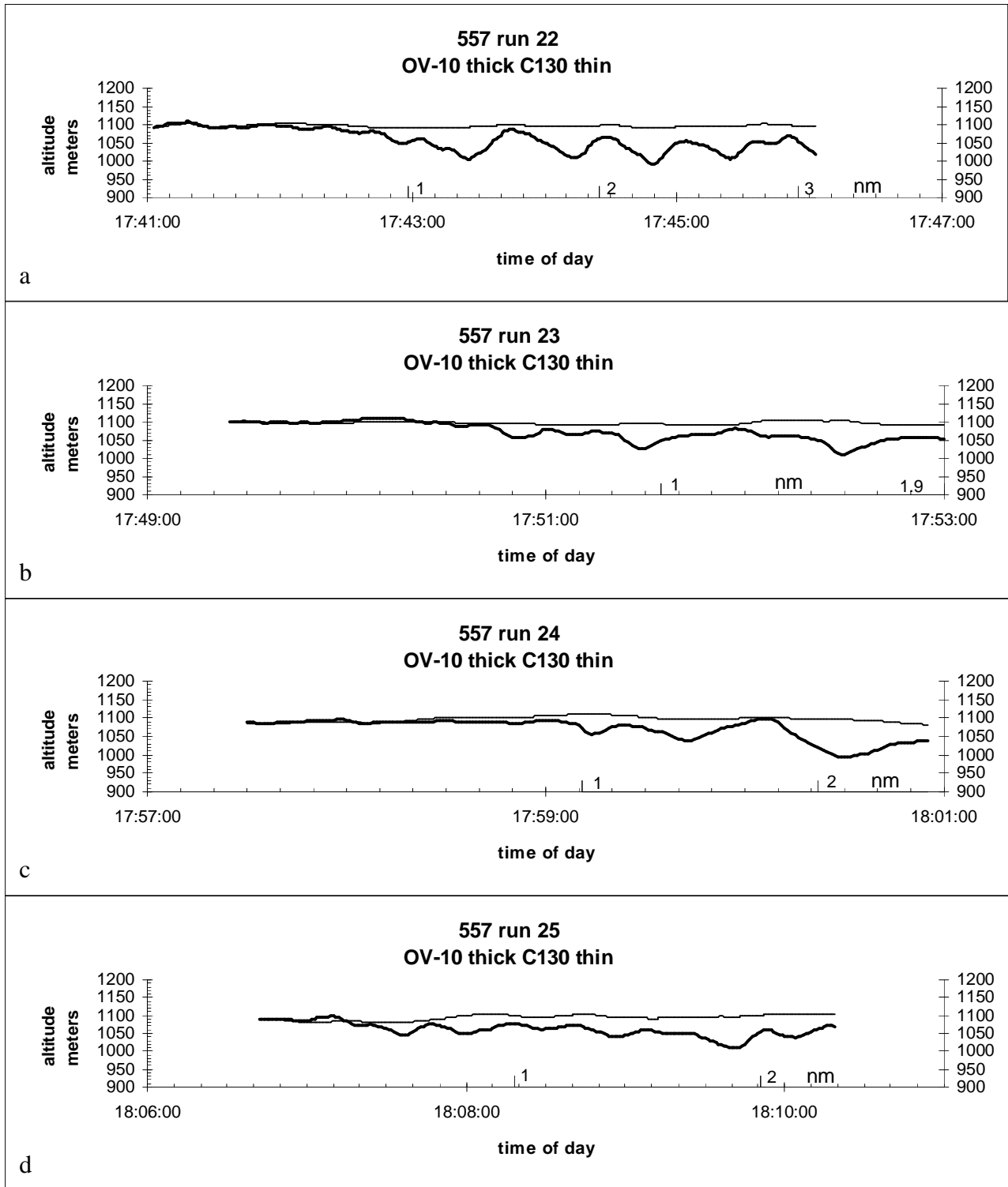


Figure 16. C130 and OV-10 GPS Altitude for Flight 557 at Run Times Shown

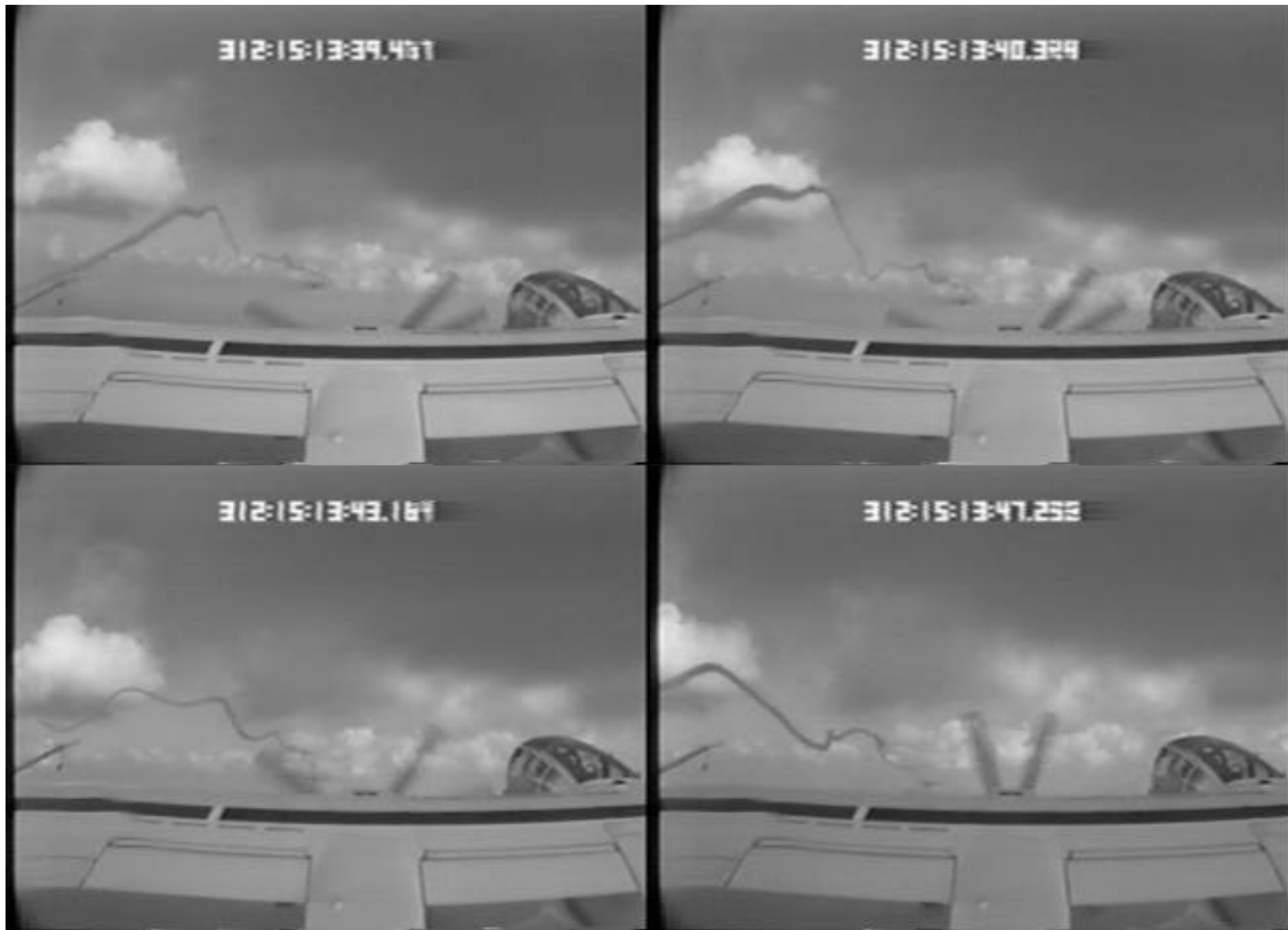


Figure 17. Video Frames From Different Times of the C130 Wake Vortex Smoke Signature